MODELING GAS KICK BEHAVIOR IN WATER AND OIL-BASED DRILLING

FLUIDS

A Thesis

by

KAUSHIK MANIKONDA

Submitted to the Office of Graduate and Professional Studies of
Texas A&M University
in partial fulfillment of the requirements for the degree of

MASTER OF SCIENCE

Chair of Committee,   Abu Rashid Hasan
Co-Chair of Committee,   Mohammad Azizur Rahman
Committee Member,   M. M Faruque Hasan
Head of Department,   Jeffrey B. Spath

August 2020

Major Subject: Petroleum Engineering

ABSTRACT[*]

       This thesis presents a semi-analytical model to simulate the behavior of a gas kick in an annulus that accounts for gas solubility in oil-based drilling fluids. This simulator examines critical kick indicators such as pit gain and wellhead pressure with time. It models the gas behavior using a drift-flux approach with bubble rise velocity appropriate for flow through an annulus. It also uses the Peng-Robison equation of state, van der Waals mixing rules, along with binary interaction coefficients appropriate for drilling fluids, to account for gas solubility in oil-based mud.

       The simulation results predict that a five-barrel (bbl.) gas kick, would reach the wellhead of a 10,000 ft deep, non-circulating, vertical well in approximately 78 minutes. But it would only take 35 minutes to traverse the same well, if the well is circulating at 702 gallons per minute. This variation in kick travel times results from the difference in the bubble translational velocity in the two cases. The average translational velocity is 2.1 ft/sec when there is no circulation, as opposed to 4.68 ft/sec, when the mud is circulating.

       The simulations also predict that if there is a constant kick influx of 1 scf/sec, the first gas bubbles would reach the wellhead of the same, non-circulating well in 4.45 hours. But only take 52 minutes when it is circulating. The bubble's shape, size, and rise velocity are the primary causes for this significant difference in kick travel time between the two

---

non-circulating cases. The single, 5 bbl. bubble travels as a Taylor bubble with an average rise velocity of 2.1 ft/sec, while the smaller bubbles in the constant influx case migrate at an average velocity of 0.64 ft/sec. Incorporating gas solubility into these simulations revealed that the choice of drilling fluid volume factor (B_o) correlation affects the results significantly. It also showed that some of the existing B_o correlations fail, for drilling fluid swelling calculations, at higher pressures and temperatures. Finally, the results indicate that a gas kick would take longer to reach the wellhead when it is soluble in the mud than when it is not, regardless of the choice of B_o correlation.

Most of the existing kick simulators either partially or entirely overlook the effects of solubility on gas migration. This model accounts for the gas kick's solubility in oil-based drilling fluids, an issue that is critical for off-shore drilling. Applicability of empirical two-phase flow correlations developed for flow in cylindrical conduits, to a gas kick situation is questionable. This simulator addresses this issue by using a semi-analytical approach for modeling two-phase flow in an annulus.

DEDICATION

I dedicate this Thesis to my courageous mother, Lakshmi Prasanna Manikonda. I will forever be indebted to her for her sacrifices, compassion, encouragement, and support. She is an inspiration to me, without whom none of my work would have been possible.

ACKNOWLEDGEMENTS

CONTRIBUTORS AND FUNDING SOURCES

Contributors

This research was supervised by a thesis committee consisting of Professors Abu Rashid Hasan [advisor], Jerome J. Schubert [co-advisor], and Mohammad Azizur Rahman [co-advisor] of the Harold Vance Department of Petroleum Engineering; and Professor Faruque Hasan of the Artie McFerrin Department of Chemical Engineering.

Dr. Nazmul Rahmani of the Wayne H. King Department of Chemical and Natural Gas Engineering at Texas A&M University, Kingsville, validated the model presented in section 6 using HYSYS. My colleague and good friend, Omer Kaldirim, contributed to the single bubble models presented in section 4. The binary interaction coefficients used in section 6, are a result of my colleague, Dr. Jian Feng's prior work. Dr. Feng, along with Dr. William McCain Jr. also contributed ideas to the solubility modeling in section 6.

All other work conducted for the thesis was completed by the student independently.

Funding Sources

NOMENCLATURE

γ_{API}	Oil API gravity, ^{o}API
$\gamma_{g,o}$	Gas, Oil specific gravity, dimensionless
ρ_g	Gas density, lbm/ft^3
ρ_L	Drilling fluid density, lbm/ft^3
ω	Acentric factor, dimensionless
$(P_G)_{n,\,n+1}$	Pit gain at the nth, and $(n+1)^{th}$ step, bbl.
$\left(\dfrac{dp}{dz}\right)_f$	Frictional pressure gradient, psi/ft
$\left(\dfrac{dp}{dz}\right)_g$	Hydrostatic pressure gradient, psi/ft
B_o	Oil volume factor, RB/STB
B_{ob}	Volume factor at the bubble point pressure, RB/STB
C_o	Flow parameter, dimensionless
c_o	Oil compressibility, psi^{-1}
$D_{1,2,n}$	Depth at point 1, point 2 and the depth at the nth step, ft
D_{BH}	Depth to the bottomhole, ft
d_i	Drillpipe outside diameter, in.
d_o	Casing inside diameter, in.
D_{WH}	Depth to the wellhead, ft
f	fugacity, psia
f_g	Gas volume fraction, dimensionless
$f_{gj,\,Lj}$	Gas phase and the liquid phase fugacity of the jth component, psia

$f_{L,g}$	Liquid, gas phase fugacity, psia
g	acceleration due to gravity, 32.2 ft/sec^2
G	Gibbs molar free energy, lbf-ft/mole
L_b	Length of the gas bubble, ft
$p_{1,2,n}$	Pressure at point 1, point 2, and the pressure at the nth step, psia
p_b	Bubble point pressure, psia
p_{BH}	Bottomhole pressure, psia
p_C	Critical pressure, psia
p_{WA}	Wellhead pressure, psia
R	Gas constant, psi-ft^3/lb mole-°R
R_s	Solution gas-oil ration, scf/STB
$T_{1,2}$	Temperature at point 1, point 2, °F
T_C	Critical temperature, °F
$V_{1,2}$	Volume at point 1, point 2, ft^3
$v_{\infty T}$	Gas bubble terminal rise velocity, ft/sec
v_g	Real velocity of the gas bubble, ft/sec
v_m	Mixture velocity, ft/sec
V_M	Molar volume, ft^3/mol
$z_{1,2}$	Z-factor at point 1, point 2, dimensionless
$z_{g,L}$	Gas, liquid phase z-factors, dimensionless

TABLE OF CONTENTS

xi

LIST OF FIGURES

LIST OF TABLES

1. INTRODUCTION [*]

An unscheduled entry of the reservoir fluids into the wellbore while drilling is called a 'Kick.' A kick happens when the pressure inside the wellbore is lower than the formation pore pressure. An unmitigated kick might lead to a Blowout. Oil and Gas well blowouts are disastrous for everyone involved. They are extremely expensive financially, environmentally, reputationally, and most important of all, in terms of the human cost. For example, on April 20, 2010, the Deepwater Horizon Oil rig in the Macondo oil prospect in the Mississippi Canyon blew out. According to the environmental protection agency, it resulted in the death of 11 workers on the Deepwater Horizon and the largest spill of oil in the history of marine oil drilling operations. 4 million barrels of oil flowed from the damaged Macondo well over an 87-day period, before it was finally capped on July 15, 2010 (Deepwater Horizon, 2017). So, it is in the best interest of everyone for a drilling engineer to be able to detect and control a kick as quickly as possible.

A kick can be of two types, an Oil kick (or liquid phase kick) and a gas kick. A gas kick is particularly dangerous because of its insidious nature. A gas kick can be difficult to detect, especially at the initial stages of its migration. However, as it reaches the wellhead, the gas expands rapidly because of the low surrounding pressure, posing great risks to the equipment and the structural stability of the drilling rig. In the Deepwater

---

Horizon example discussed earlier, a surge of Natural gas from an inadequate cement core could have caused the blowout.

1.1. Objective and Scope of the Research

The primary objective of this research project was to develop a semi-analytical model to simulate the behavior of a gas kick in water and oil-based drilling fluids. The model considered the following two relatively simple situations:

1. Single gas bubble kick migration

2. Kick migration with a constant gas influx

Each of these two cases has two more sub-scenarios, namely, with circulation, and without any circulation in the annulus. So, in total, the model studied the following four situations for both aqueous and oil-based drilling fluids:

1. Single gas bubble kick migration

    a. Single gas bubble kick migration with no circulation in the annulus

    b. Single gas bubble kick migration with circulation in the annulus

2. Kick migration with a constant gas influx

    a. Kick migration with a constant gas influx rate and with no circulation in the annulus

    b. Kick migration with a constant gas influx rate in a circulating annulus

Section 4 of this thesis discusses the two single bubble kick migration cases, while section 5 deals with both constant kick influx cases.

1.2. Modeling Approach

The model used the drift-flux approach to simulate two-phase flow in vertical and inclined annuli presented by Hasan and Kabir (1992). Scenarios 2a and 2b used this approach to model the two-phase flow resulting from a continuous inflow of a gas kick. Cases 1a and 1b used the Taylor bubble rise velocity appropriate for an annulus (Hasan and Kabir, 2018) to simulate a single bubble gas kick migration. The model then used the Peng-Robinson equation of state (Peng et al., 1976), to enable all four cases to account for gas solubility in oil-based drilling fluids. The integration of the Peng-Robinson equation into the gas kick models required the use of Van der Waal's mixing rules as presented by Kwak et al. (1986). It also needed utilizing binary interaction coefficients suitable for drilling fluids.

Gas solubility in oil changes the volume of oil. Expressions used to represent this volume change as a factor of dead oil volume, B_o, affect the results of the simulation significantly. Hence, it is vital to select the appropriate B_o correlation for high-pressure situations such as a deep-water drilling operation. The oil volume factor correlations investigated in these models are those by Standing, (1947), Petrosky & Farshad (1993), and Vazquez & Beggs, (1977).

All four cases investigated two key kick indicators, the pit gain (increase in mud volume in the mud pit) observed and the change in wellhead annulus pressure (WHAP). Thomas et al. (1984) studied the effects of gas solubility in oil-based drilling fluids on kick detection. They concluded that pit gain is the most reliable indicator of a kick during

3

drilling in both oil and water-based drilling fluids. So, we selected pit gain to be one of

two key indicators to be studied through these models.

2. EXISTING KNOWLEDGE AND ADDITIVE INFORMATION[*]

This section discusses the work done previously by other researchers in the areas of gas solubility in drilling fluids, gas kick simulation, and gas bubble rise velocity in a kick situation. It examines the strengths and limitations of the existing knowledge on the topic. It also analyzes how the models presented in this thesis tried to improve upon these current simulators. This section branches into various sub-sections based on the specific area of study under consideration. These individual sub-sections discuss the strengths, limitations, and attempts at betterment made in these areas.

2.1. Gas Solubility in Oil-based Drilling Fluids

Most of the current kick simulators either partially or entirely overlook the effects of solubility on gas migration. An issue that is critical for offshore drilling because of the rapid changes it produces close to the wellhead. O'Bryan (1988) studied the complications posed by gas solubility in drilling fluids to well-control operations. The paper presented results from experimental studies conducted in a 6000 ft test well. O'Bryan developed an empirical correlation to estimate the solubility of methane, ethane, and CO_2 in oil-based drilling fluids from these experimental studies. He also presented an equation of state model using Peng-Robinson EOS to predict gas solubility. The paper compared the results

from the experimental studies with those from the EOS model and found acceptable agreement.

Thomas et al. (1984) also studied the effects of dissolution of gas on the properties of non-aqueous drilling fluids. Their methane solubility calculations in drilling mud mixtures, used the Redlich-Kwong equation of state (1949) along with the correlations developed by Yarborough et al. (1978). Thomas et al. (1984) also carried out experimental studies to measure gas solubility if oil-based drilling fluids. They adjusted the ARKES binary interaction parameters, C_{ij} to 0.061 to fit their experimental phase equilibrium data over a wide range of compositions. They developed a blowout simulator using their gas solubility models and contemporary gas-bubble rise velocity equations.

Manikonda et al. (2020), developed a thermodynamic method for estimating drilling fluid swelling (B_o) from gas dissolution. They advance the models presented in this thesis, and Manikonda et al. (2019), and layout a detailed procedure to calculate solution gas-oil ratio (R_s) in kick situations. They validate their results using Aspen HYSYS, a commercial chemical process simulation software.

Although empirical correlations are beneficial and can save time, their applicability is limited. Because of their inherent nature, the applicability of empirical correlations outside of their original data set is often ambiguous. So, the gas solubility equation proposed by O'Bryan (1988) does not apply to every kick situation. The approach followed by Thomas et al. (1984), however, minimizes this issue by using the Redlich-Kwong equation of state (1949) for their solubility models. However, the bubble rise velocity research available at that time constrained their blowout simulator. Moreover,

they did not make any attempts to simulate a gas kick with a variable or constant gas influx.

Research presented in this thesis addresses these two problems by combining the semi-analytical approach, followed by Thomas et al. (1984) with a variety of kick situations. As mentioned earlier, this thesis considers four distinct kick situations and uses the Peng-Robinson EOS to model gas solubility in drilling fluids. Also, an abundance of research about gas-bubble rise velocity in an annulus is available today, most notably Hasan-Kabir (2018). The next subsection discusses the advancements made in this area since 1984.

2.2. Gas Bubble Rise Velocity in Kick Situations

Rader et al. (1975) carried out experiments to understand the major factors affecting the bubble rise velocity in an annulus. They concluded that the geometry of the annulus is the most important factor influencing the rise velocity. They also concluded that liquid viscosity, gas, and liquid densities, liquid velocity, and the angle of vertical deviation also have a significant impact on the rise velocity. However, they stated that the length of the bubble, the eccentricity of the annulus, and the surface tension between the gas and the liquid have little effect on the velocity.

Kaldirim & Schubert (2017) conducted an experimental study of riser gas behavior in a small-scale set-up. They used a 27 ft. tall, 6 in. clear PVC pipe encompassing a 2 in. white PVC pipe to simulate a riser system. They used the 2-in. PVC pipe as a drill pipe, to feed their system with mud and circulate it through the riser annulus. They injected gas

at the base of this set-up and measured the difference in the amount of gas entering and exiting this riser system. They concluded that a single Taylor bubble kick could be dispersed into a regional bubbly flow by increasing the mud flow rate. They also observed that the geometry of the outflow line could influence the gas flow behavior significantly.

Kaldirim & Schubert (2018) continued their work from Kaldirim & Schubert (2017) and modified their experimental set-up to observe riser gas expansion in a vacuum. They installed a vacuum pump at the top of the configuration previously described, to mitigate the effects of atmospheric pressure and to compensate for the short length of their system. After repeating their experiments in the new system, they reported that when they reduced the pressure at the top to 1.95 psia, the gas bubble expanded to almost twice its original volume during its migration from the base to the top of the flow loop.

Johnson & White (1991) conducted gas migration experiments in a 49 ft tall flow loop with a 7.8 in. ID pipe. They used Xanthan gum solution to emulate drilling mud and air as the gas phase. They observed that gas bubbles migrate quicker in viscous drilling fluids than in water, a surprising result at the time (but consistent with field observations). They concluded that most of the existing kick simulators at the time significantly underestimated the rise velocity of gas bubbles and predicted delayed gas arrival times. They recommended further research into the effects of annular geometry on bubble rise velocity.

Skalle et al. (1991) conducted similar experiments but on a much larger scale. They used a 500 ft vertical well with a 2.93 in. annulus to study two-phase flow in flowing and stagnant liquid columns. They concluded from their results that the C_o value of 1.2 was

the most appropriate for dispersed bubbly and Slug flows. That was in sound agreement with other presented research at the time.

Hasan and Kabir (2018) proposed a modified Taylor bubble rise velocity equation for flow through an annulus. All the simulations presented in this thesis used this equation to model rise velocity and Hasan-Kabir (1992) drift-flux approach to simulate two-phase flow through an annulus.

2.3. Gas Kick Simulation

Moving on to existing kick simulators, Chukwudi et al. (2017) and Chukwudi et al. (2018) developed a kick simulator. They incorporated the effects of fluid compressibility, annular friction pressure loss, choke line friction pressure loss, temperature, variable fluid density, and two-phase flow into their model. Their model used the continuity equation along with the equation of state to develop the simulator. They modeled the effects of gas migration using Harmathy (1960), and Zuber et al. (1965) bubble rise velocity models. They used the Beggs and Brill (1973) correlation to model two-phase flow in an annulus. However, the applicability of empirical two-phase flow correlations like Beggs and Brill developed for flow in a cylindrical conduit, is questionable for modeling two-phase flow in an annulus. The absence of gas solubility discussions in their simulation limits its applicability in offshore operations.

Ma et al. (2018) used a transient drift-flux approach built on mass and momentum conservation to simulate gas kicks in oil-based drilling fluids. They used the correlation developed by Monteiro et al. (2010) to calculate methane solubility at a specific

temperature and pressure in oil-based drilling fluids. They employed advanced numerical schemes to handle the mass transfer between the liquid and gas phases. They found that the gas was dissolved entirely in the mud at bottom hole conditions and this delayed kick detection significantly. They also concluded that because of this delay in detection caused by the dissolution of gas, drilling crews would have a very short window to react to a kick. The models proposed in this thesis aim to do something similar but using a semi-analytical (less time-consuming) approach.

Chandrasekaran et al. (2019) developed a mathematical1-D two-phase flow model to simulate a gas kick flow system during vertical drilling. They employed a drift-flux approach where they assumed that average mixture properties represent the fluid properties. They predicted the kick velocity and pressure in the annulus at the bit based on surface flow measurements in real-time drilling. They concluded that their model could be employed in real-time drilling to model influx events.

Numerical and mathematical simulations such as Chandrasekaran et al. (2019), and Ma et al. (2018) are an excellent tool to model complex phenomena. However, a driller's ability to customize these models to a specific situation is limited by these models' inherent nature. Unlike analytical and semi-analytical models, numerical ones provide a limited understanding of the physical phenomena involved. When the simulation fails, it can be very tedious to go through the motions of debugging for mathematical models. In a time-sensitive situation like a gas kick, doing something like that might not be an option. Also, numerical simulations are notorious for taking very long to execute. The models in

this thesis address these issues by following a semi-analytical approach. Hence, they are much easier to run, comprehend, and customize.

3. BASE CASE AND ASSUMPTIONS

The base case for all the models in this thesis is a hypothetical 10,000 ft deep vertical well, with a 4.5 in. drillpipe outside diameter (OD), and a 12.415 in. casing inside diameter (ID). The entire length of the wellbore is assumed to continue at the same diameter as the casing ID. The surface and bottomhole temperatures are 50 degrees Fahrenheit (ºF), and 302 ºF respectively, and the temperature is assumed to increase linearly with depth (geothermal gradient). Modeling heat transfer between the fluids is beyond the scope of this research. Therefore, the temperature at every point in the wellbore is assumed to be the same as the outside temperature at that depth. The " Limitations and Recommendations for future work" section discusses the limitations and possible remedies of this assumption in detail.

The density of the drilling fluid in use is 10 pounds per gallon (lbm/gal), and its composition varies, depending on the specific case under consideration. For example, it is a water-based mud (WBM), for scenarios without any gas solubility, and an oil-based mud (OBM) for others. The circulation rate of the mud, when there is any circulation, is 702 gallons per minute (gal/min). All scenarios consider the effects of mud compressibility to be negligible for all modeling purposes. Other drilling fluid properties such as the fluid viscosity, surface tension, composition (for OBM), etc. are presented in appendix A.

The gas kick is assumed to contain pure methane to simplify solubility modeling. The volume and influx rate of the gas kick depends on the individual scenario, and each case's sub-section discusses these details at the beginning. All four instances assume a

constant bottomhole pressure (BHP) throughout the whole process. The assumption is that the Driller's method for well control is in use, and the driller is managing to maintain a steady BHP throughout the kick migration process. This assumption is not always practical, and gas migration usually tends to affect BHP. Discussion about the limitations and possible future remedies of these two assumptions are also in the "Limitations and Recommendations for Future Work" section.

It should be noted that all the variables assumed here such as the well depth, annular diameter, mud-weight, etc. can be adjusted to customize this simulator to specific drilling conditions.

4. SINGLE BUBBLE KICK MIGRATION IN AQUEOUS DRILLING FLUIDS[*]

This section discusses the two single bubble kick migration cases in WBM, (scenarios 1a and 1b) as referenced in sub-section 1.1. These two cases assume that the single bubble entering the wellbore travels up in the annulus as a Taylor bubble (Slug).

4.1. Single Bubble Kick Migration with No Mud Circulation in the Annulus

A gas kick of volume 5 barrels (bbl.) at bottomhole conditions entered the wellbore at 10,000 ft. There is no further gas influx and no drilling fluid circulation in the annulus. The gas bubble starts migrating up the length of the annulus and expanding in the process. This hypothetical scenario might arise when a drilling engineer suspects a gas kick and halts drilling to analyze the situation. As mentioned earlier, this simulation assumes that the driller successfully maintains a steady BHP throughout the process and studies the changes in pit gain and wellhead annulus pressure (WHAP).

4.1.1. Modeling

As the gas bubble starts rising in the annulus, the decrease in hydrostatic pressure causes it to expand. However, the presence of drilling mud both above and below the gas bubble restricts its expansion. The degree of expansion of the gas bubble and the pressure

---

at the bubble's location are interdependent variables. When the bubble travels from point one to point two, how much its volume increases depends on the pressure difference between the two points. But, the pressure difference between the two locations also depends on the height of the gas kick, which is directly proportional to its volume. More precisely, when the bubble moves between those two points, it is replacing the original heavy drilling mud between them with itself (lighter methane gas). This replacement results in a smaller hydrostatic pressure drop between the locations and higher pressure at point two than before. Another way to express this idea in simpler terms is, as the gas bubble rises, it carries excess pressure with it and adds it to its new location. The following equations express this idea mathematically:

$$p_2 = p_1 + \left(D_1 - D_2 - \frac{L_b}{2}\right)\left[\left(\frac{dp}{dZ}\right)_{g\ mud}\right] + \left(\frac{L_b}{2}\right)\left[\left(\frac{dp}{dZ}\right)_{f\ avg\ gas} + \left(\frac{dp}{dZ}\right)_{g\ gas}\right] \quad (1)$$

$$L_b = \frac{V_2}{Annular\ Capacity} \quad (2)$$

$$V_2 = V_1 * \left(\frac{p_1}{p_2}\right) * \left(\frac{T_2}{T_1}\right) * \left(\frac{z_2}{z_1}\right) \quad (3)$$

This case ignores the frictional pressure gradient for the drilling fluid because there is no mud circulation in the annulus. Frictional pressure drop, a minor factor even with mud circulation, diminishes further when it is a standing liquid column. The simulator uses only half of the gas bubble length (L_b) because it assumes that the center of the bubble is at point two when executing these calculations. This assumption allows the simulator to use the pressure at point two as the mean pressure throughout the length of the bubble.

The simulator deals with this interdependency issue by following an iterative approach. It divides the well into one hundred equally spaced elements and develops an initial pressure and temperature profile for the entire system. It then uses this initial hydrostatic pressure at each elemental depth to calculate a theoretical volume for the gas bubble (V_2), if the bubble were to exist at that depth and pressure. This volume is then used to estimate the theoretical height of the bubble (L_b) at each elemental depth. Then, the simulator takes this bubble height to develop a new pressure profile for the entire system. The process is then repeated using the latest pressure profile and the gas bubble volume. This cycle continues multiple times until the pressure values converge at each of these elemental depths.

The theoretical gas volumes, calculated during the iterative step where the pressure values converge, give us the real gas bubble volumes at each elemental depth. The pit-gain (P_G) observed by the driller at the wellhead, is just higher than expected amounts of drilling fluid being returned by the gas expansion. Hence, the pit-gain when the gas bubble is at different elemental depts is calculated using the following equation:

$$(P_G)_{n+1} = (P_G)_n + (V_{n+1} - V_n) \qquad (4)$$

$$\lim_{n \to 0} (P_G)_n = 5 \text{ bbl} \qquad (5)$$

where V_n, and V_{n+1} are the gas bubble volumes at the nth and $n+1^{th}$ steps respectively.

The wellhead annulus pressure (WHAP) depends heavily on the height of the gas bubble in the annulus. The longer the length of the bubble, the smaller the pressure drop between the bottomhole and the wellhead and the higher the WHAP. Mathematically, it is calculated using the following equation:

$$(p_{WA})_{n+1} = p_{BH} + (D_{BH} - (L_b)_{n+1}) \left[\left(\frac{dp}{dZ}\right)_{g\ mud} \right] + (L_b)_{n+1} \left[\left(\frac{dp}{dZ}\right)_{f\ avg\ gas} + \left(\frac{dp}{dZ}\right)_{g\ gas} \right]_n \qquad (6)$$

Since the model assumes a Taylor bubble for kick migration, the following equation (Hasan & Kabir, 2018) gives the bubble rise velocity at different elemental lengths:

$$v_{\infty T} = (0.35 + \frac{0.1 d_i}{d_o}) \sqrt{(g d_o * (\rho_L - \rho_g)/\rho_L}} \qquad (7)$$

Where d_i is the drillpipe OD and d_o is the casing ID.

4.1.2. Results

Simulation results show that a 5-bbl. gas kick would reach the wellhead in approximately 78 minutes under the model's conditions. It would expand to about five times its original volume and produce a total pit gain of 25.6 bbl. It would cause the wellhead annulus pressure to increase from 532 psia to 614 psia in those 78 minutes. The bubble's terminal rise velocity would increase from approximately 2 feet per second (ft/sec) at bottomhole conditions to 2.2 ft/sec near the wellhead. The plots 4.1- 4.3 below depict these results graphically.
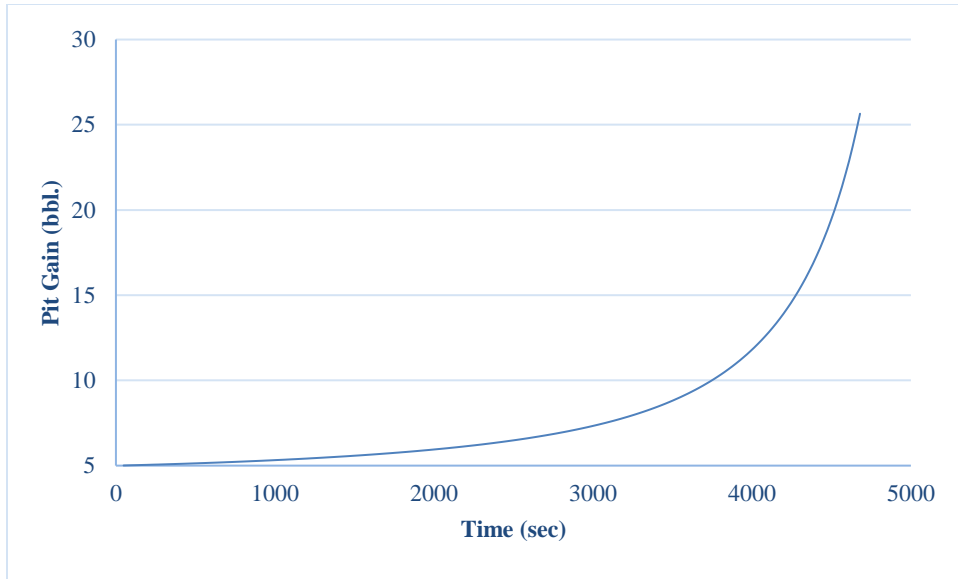
Figure 4.1 Pit gain vs Time plot for a single 5 bbl. gas bubble.
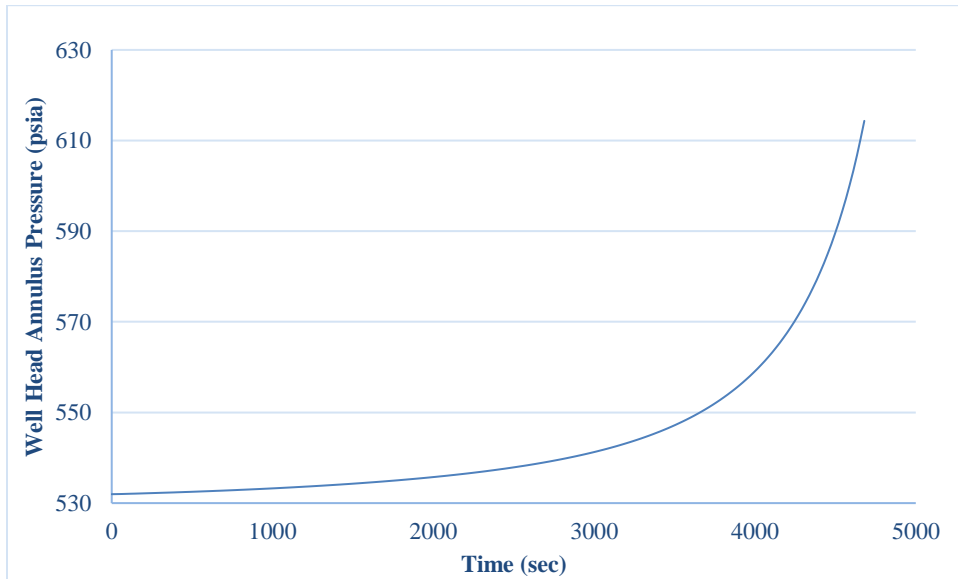
Figure 4.2 Wellhead annulus pressure vs Time plot for a single 5 bbl. gas bubble.
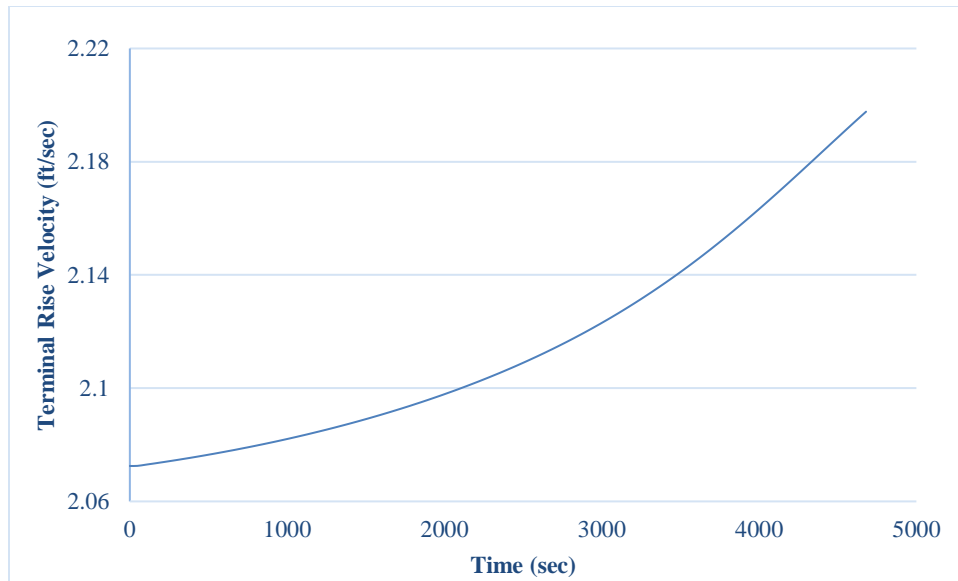
Figure 4.3 Terminal rise velocity vs Time plot for a single 5 bbl. gas bubble.

4.1.3. Sensitivity Analysis

This section compares the results for three different initial gas bubble sizes, 0.5-, 5-, and 8 bbl. All other simulator conditions, such as the well depth, mud-weight, inclination, etc. are the same as the base case. The results show that a 0.5 bbl. initial influx would expand approximately 5.6 times and produce a total pit gain of 2.78 bbl. Whereas the 5-, 8 bbl. bubbles expand to about five times and 4.9 times respectively. Following a similar pattern, the 0.5 bbl. bubble increases the WHAP by approximately nine psia whereas the 5-, 8 bbl. influxes increase it by 82 psia and 125 psia respectively. On the other hand, the bubble rise velocity for all three bubbles follows almost the same path and varies slightly to the end. Hence, all three bubbles take approximately the same time to reach the wellhead.
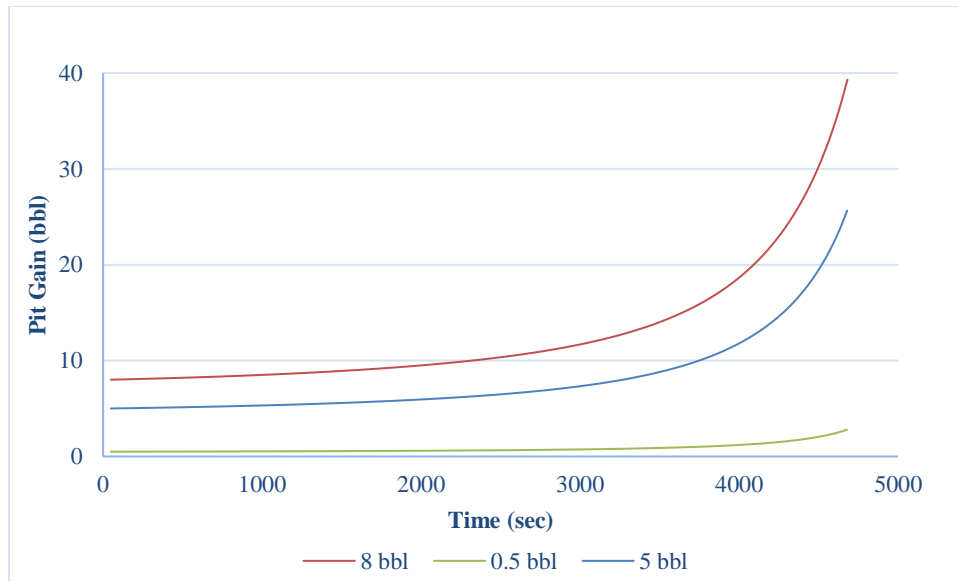
Figure 4.4 Pit gain vs Time plots comparison among different initial kick sizes.

One interesting observation from Fig. 4.4 is that the smaller 0.5 bbl. bubble expands to 5.6 times its original volume, while the larger bubbles expand to only around 5 times. In fact, as the initial bubble size increases, the factor of expansion decreases slightly. One possible explanation for this pattern might be the earlier discussed height-pressure relationship. The larger bubble's tendency to replace more mud in the annulus is restricting its expansion by maintaining higher pressure at its position, as shown in Fig. 4.5 below.
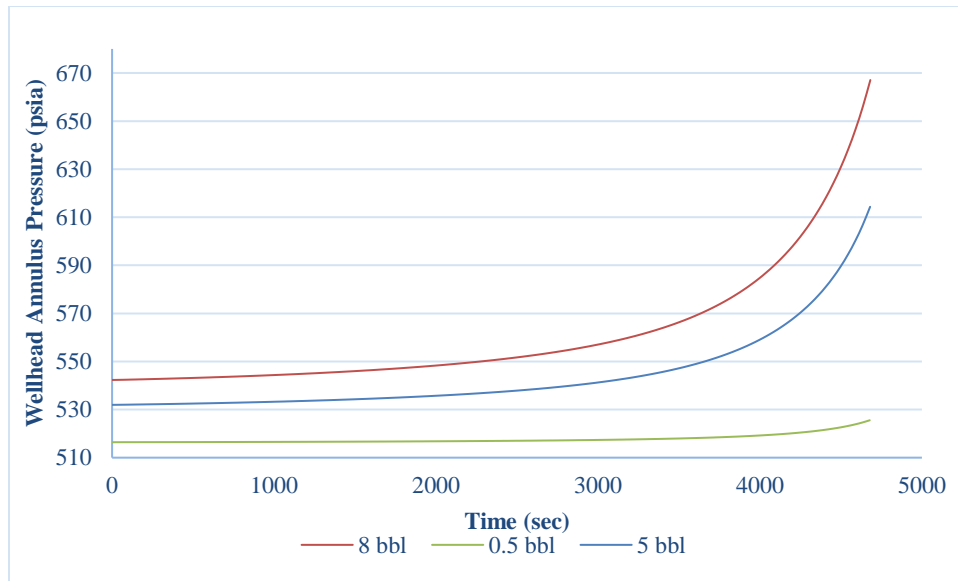
Figure 4.5 Wellhead annulus pressure vs Time plots comparison among different initial kick sizes.

4.2. Single Bubble Kick Migration with Mud Circulation in the Annulus

A gas kick of volume 5 barrels (bbl.) at bottomhole conditions entered the wellbore at 10,000 ft. There is no further gas influx, and the drilling fluid is circulating at a rate of 702 gal/min in the annulus. This hypothetical scenario might arise when a drilling engineer is trying to circulate a kick out of the annulus.

4.2.1. Modeling

This case is very similar to the one discussed in the previous sub-section, except for the added drilling fluid circulation. So, the same interdependency problem exists here, and the simulator employs the same iterative strategy to deal with it. Most of the equations used for the last case are also applicable here, except for equations 1, and 6. The modifications required for these two equations to make them suitable here are:

21

$$p_2 = p_1 + \left(D_1 - D_2 - \frac{L_b}{2}\right)\left[\left(\frac{dp}{dZ}\right)_{g\ mud} + \left(\frac{dp}{dZ}\right)_{f\ mud}\right] + \left(\frac{L_b}{2}\right)\left[\left(\frac{dp}{dZ}\right)_{f\ avg\ gas} + \left(\frac{dp}{dZ}\right)_{g\ gas}\right] \quad (8)$$

$$(p_{WA})_{n+1} = p_{BH} + (D_{BH} - (L_b)_{n+1})\left[\left(\frac{dp}{dZ}\right)_{g\ mud} + \left(\frac{dp}{dZ}\right)_{f\ mud}\right] + (L_b)_{n+1}\left[\left(\frac{dp}{dZ}\right)_{f\ avg\ gas} + \left(\frac{dp}{dZ}\right)_{g\ gas}\right]_n \quad (9)$$

Because there is mud circulation in the annulus, the model cannot ignore the frictional pressure drop from the drilling mud. The additional pressure gradient term in the above two equations corrects them for this frictional pressure drop.

Another way this model differs from the previous case is in terms of the real bubble velocity. When there is no mud circulation in the annulus, the bubble's rise velocity is also its real velocity. However, when there is mud circulation, the real velocity would be the sum of its rise velocity and a fraction of the mixture velocity. The rise velocity of the gas bubble alone is still estimated using the same equation as before (Hasan & Kabir, 2018). But, the real velocity of the bubble in the system is given by the following equation:

$$v_g = C_0 v_m + v_{\infty T} \quad (10)$$

C_o is a flow distribution parameter that corrects the velocity equation for non-uniform flow distribution. The simulator uses a C_o value of 1.2, as proposed by Hasan and Kabir, 2018.

4.2.2. Results

Simulation results show that a 5-bbl. gas kick would reach the wellhead in approximately 35 minutes under this model's conditions. It would expand to a little more than five times its original volume and produce a total pit gain of 26.5 bbl. It would cause

the wellhead annulus pressure to increase from 513 psia to 596 psia in those 35 minutes. The bubble's real velocity would increase from approximately 4.64 ft/sec at bottomhole conditions to 4.77 ft/sec near the wellhead. The plots 4.6 – 4.8 below depict these results graphically.
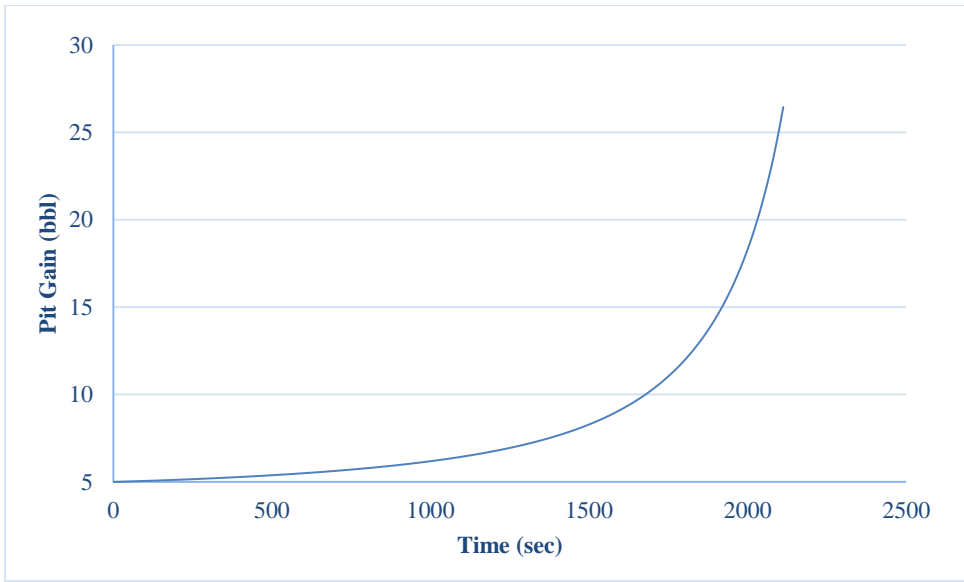
Figure 4.6 Pit gain vs Time plot for a single 5 bbl. gas bubble, in a circulating annulus.
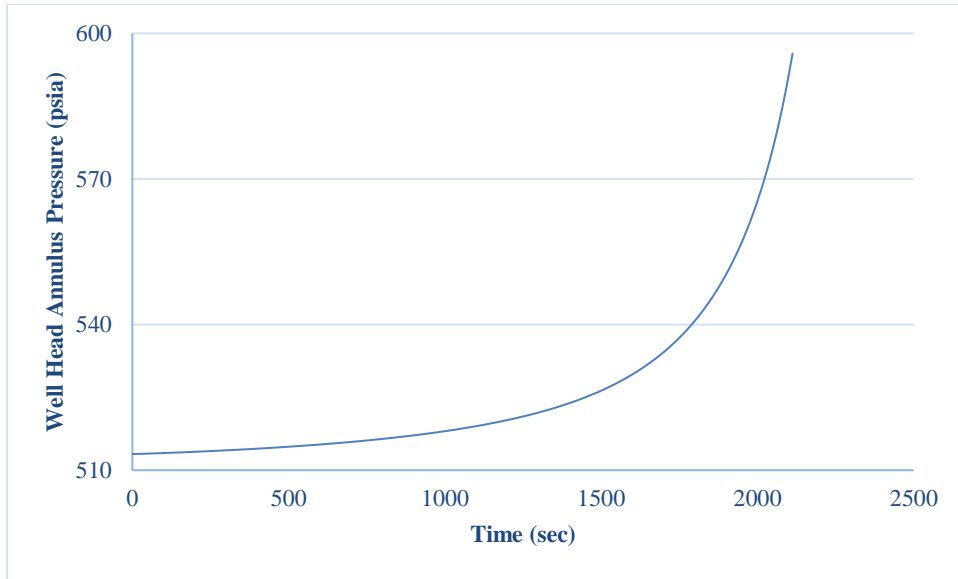
Figure 4.7 Wellhead annulus pressure vs Time plot for a single 5 bbl. gas bubble, in a circulating annulus.
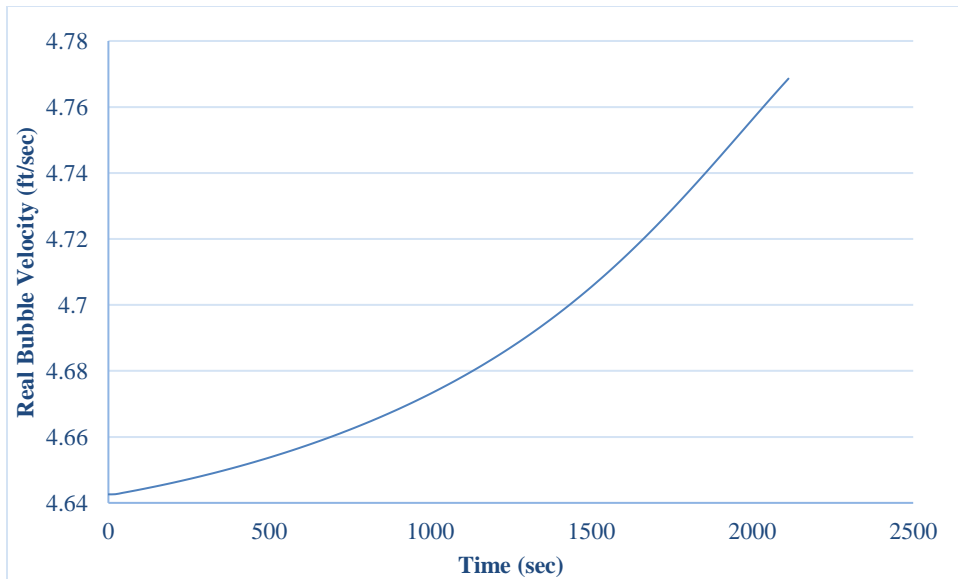
Figure 4.8 Real bubble velocity vs Time plot for a single 5 bbl. gas bubble, in a circulating annulus.

4.2.3. Sensitivity Analysis

This section compares the results for three different initial gas bubble sizes, 0.5-, 5-, and 8 bbl. All other simulator conditions, such as the well depth, mud-weight, inclination, etc. remain the same. The results show that a 0.5 bbl. initial influx would expand approximately 5.8 times and produce a total pit gain of 2.88 bbl. Whereas the 5-, 8 bbl. bubbles expand to about 5.3 times and five times respectively. Following a similar pattern, the 0.5 bbl. bubble increases the WHAP by approximately 6.3 psia while the 5-, 8 bbl. influxes increase it by 83 psia and 123 psia respectively. On the other hand, the bubble rise velocity for all three bubbles follows almost the same path and varies slightly to the end. Hence, all three bubbles take approximately the same time to reach the wellhead. Graphical representation of these results is in Figs. 4.9 and 4.10 below.
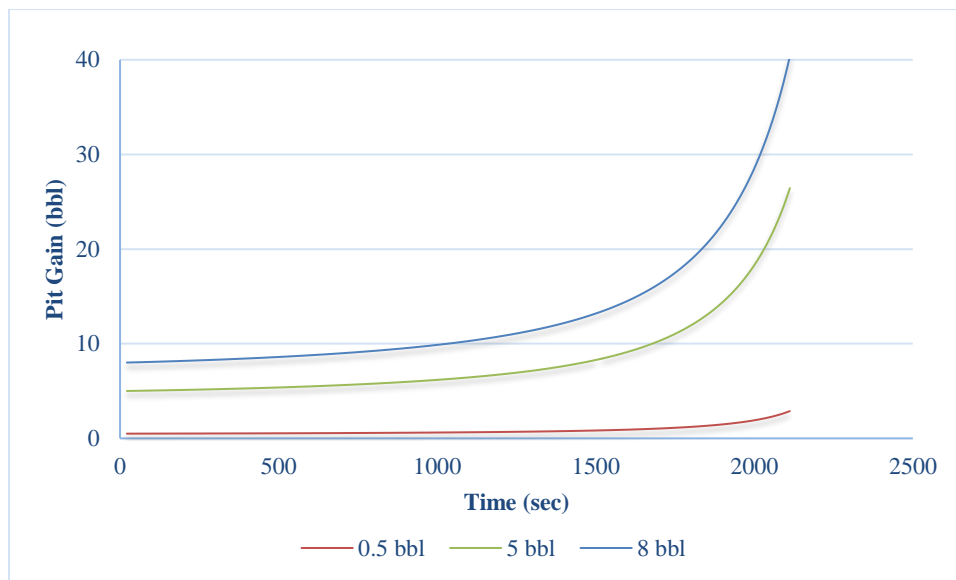
Figure 4.9 Pit gain vs Time plots comparison among different initial kick sizes, in a circulating annulus.
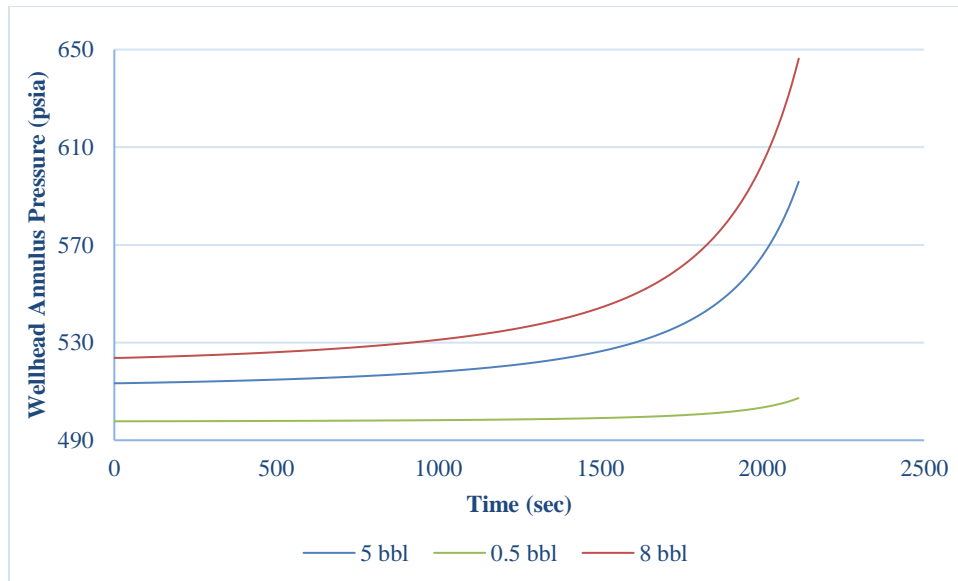
Figure 4.10 Wellhead annulus pressure vs Time plots comparison among different initial kick sizes, in a circulating annulus.

4.3. Comparison between the Cases with and without Circulation in the Annulus

Comparing the two cases in Figs. 4.11- 4.14 shows that when there is circulation in the annulus, the gas kick would reach the wellhead in less than half the time it takes for no circulation case. The gas bubbles expand slightly more when there is mudflow than they do when there is none. So, practically speaking, a drilling crew may have less than half the time to deal with a similar-sized gas kick in a circulating annulus than they do in a stagnant one.
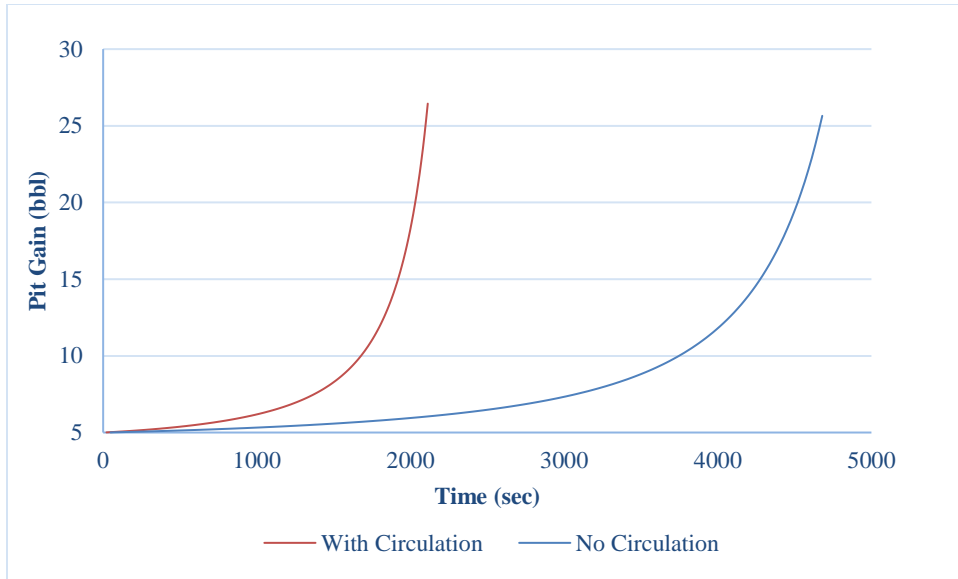
Figure 4.11 Pit gain vs Time plots comparison between the cases with and without any circulation, for a single 5 bbl. initial kick influx.
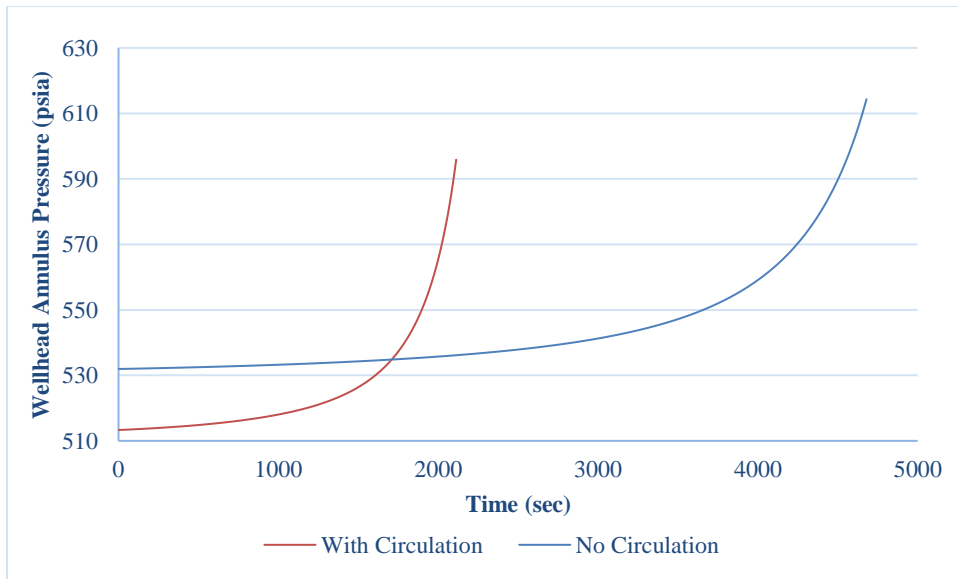
Figure 4.12 Wellhead annulus pressure vs Time plots comparison between the cases with and without any circulation, for a single 5 bbl. initial kick influx.

27
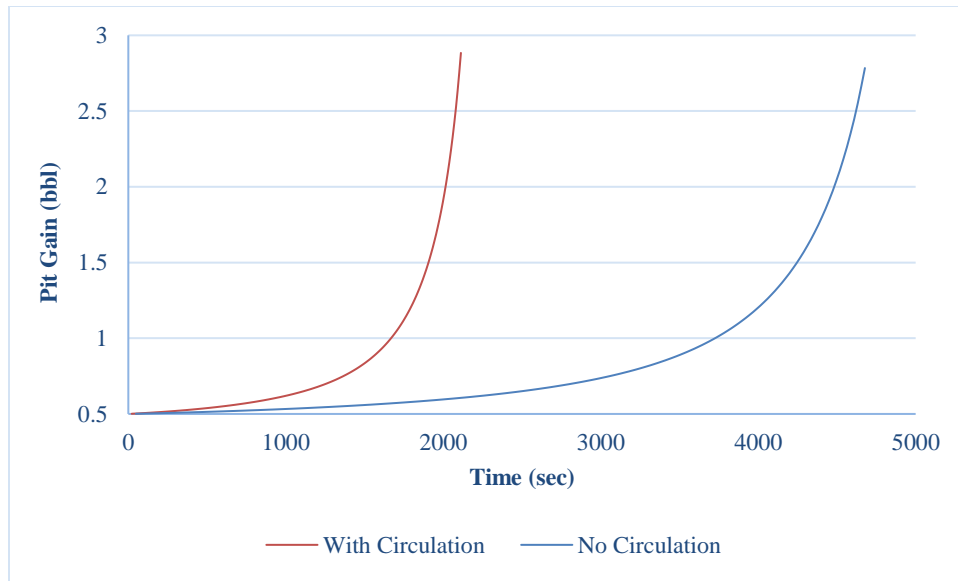
Figure 4.13 Pit gain vs Time plots comparison between the cases with and without any circulation, for a single 0.5 bbl. initial kick influx.
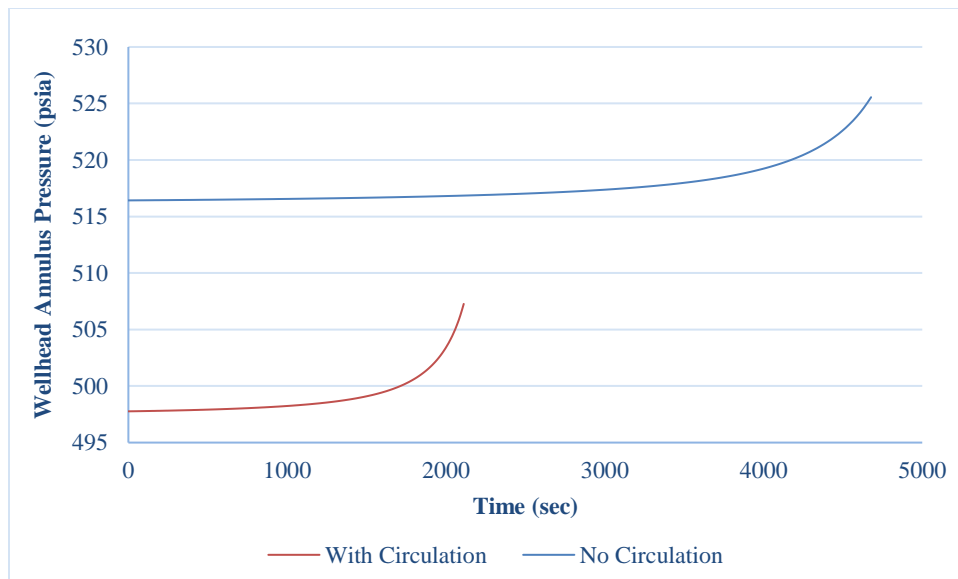
Figure 4.14 Wellhead annulus pressure vs Time plots comparison between the cases with and without any circulation, for a single 0.5 bbl. initial kick influx.

5. KICK MIGRATION IN AQUEOUS DRILLING FLUIDS WITH A CONSTANT GAS INFLUX[*]

This section discusses the two constant gas kick influx cases in WBM, (scenarios 2a and 2b) as referenced in sub-section 1.1. These two cases assume that the constant influx of the gas kick into the annulus produces a two-phase flow region.

5.1. Constant Gas Influx Kick Migration with No Mud Circulation

Gas is leaking into the well at a constant rate of 1 standard cubic foot per second (scf/sec) at 10,000 ft. There is no mud circulation in the well. As the first gas molecules enter the wellbore, the initial standing liquid in the annulus transitions into a two-phase flow. The region above the first gas bubbles is still a standing liquid column, but the flow everywhere below the highest point reached by the gas kick is a two-phase flow region. This gas inflow rate when corrected for bottomhole conditions is approximately 0.0041 cubic feet per second (ft3/sec). For context, it would take 1.9 hours to produce a 5-bbl. gas bubble at this flow rate. This hypothetical could happen when the drilling stops, and the BHP is being maintained at a constant, but inadequate levels.

---

[*] Parts of this section are reprinted with permission from "Manikonda, K., Hasan, A. R., Kaldirim, O., Schubert, J. J., & Rahman, M. A. (2019, October 13). Understanding Gas Kick Behavior in Water and Oil-Based Drilling Fluids. Society of Petroleum Engineers." doi:10.2118/198069-MS

5.1.1. Modeling

This simulator uses the Hasan-Kabir model, (Hasan & Kabir, 2018) to simulate two-phase flow in the annulus. It follows the first gas bubbles that enter the well and develops a pressure profile for the flow everywhere below these initial molecules. Pressure drop in the annulus, above these first bubbles, is the hydrostatic pressure drop of the drilling mud alone. The equations used to model two-phase flow are presented in appendix B.

Previous sections discussed the problems posed by Height-pressure relationship for single bubble cases. A similar problem exists in the constant kick influx cases as well. Because there is a continuous influx of gas, the new incoming bubbles increase the pressure above them and hinder the expansion and migration of their predecessors. As time passes and more gas comes in, the pressure drop decreases in the two-phase flow region, and the pressure increases everywhere above the bottomhole. The simulator deals with this issue by diving the well into 100 equal length segments and developing a pressure profile below the first gas bubbles, using a step-iterative approach. For the first iteration, it generates a pressure profile for the two-phase flow region, by using the flow values such as the gas void fraction (f_g), pressure gradient, etc. from the previous depth. For example, to calculate the new pressure at 9,900 ft, the simulator uses the f_g, and pressure gradient values at 10,000 ft depth. Then, for subsequent iterations, the average values between 10,000 ft and 9,900 ft are used to create new profiles. This Iteration process continues until the pressure values satisfactorily converge at all depths above the bottomhole. Mathematically, these iterations are as follows:

$$p_{n+1} = p_n + (D_n - D_{n+1})\left[\left(\frac{dp}{dZ}\right)_{g,mix} + \left(\frac{dp}{dZ}\right)_{f,mix}\right]_n \tag{11}$$

$$p_{n+1} = p_n + \frac{(D_n - D_{n+1})\left\{\left[\left(\frac{dp}{dZ}\right)_{g,mix} + \left(\frac{dp}{dZ}\right)_{f,mix}\right]_n + \left[\left(\frac{dp}{dZ}\right)_{g,mix} + \left(\frac{dp}{dZ}\right)_{f,mix}\right]_{n+1}\right\}}{2} \tag{12}$$

$$\lim_{n \to 0} p_n = p_{BH} \tag{13}$$

Eq (11) is used for the first iteration, while eq (12) is used for subsequent iterations

After developing the pressure profile, the pit gain produced by the gas is calculated using the gas void fraction at different elemental depts. Because the gas bubbles are replacing the original mud in their position, the sum of the volumes occupied by the bubbles between all elemental lengths gives the total pit gain. Mathematically, pit gain is calculated using:

$$(P_G)_{n+1} = (P_G)_n + \left[\left\{\frac{\left[(f_g)_{n+1} + (f_g)_n\right]}{2}\right\}(D_n - D_{n+1})(annular\ capacity)\right] \tag{14}$$

$$\lim_{n \to 0}(P_G)_n = 0\ \text{bbl.} \tag{15}$$

The wellhead pressure (WHAP) in this case, depends on the pressure calculated using the step-iterative approach. The flow profile produced using this approach gives the pressure at each elemental depth when the first gas bubbles reach that depth. So, the wellhead pressure, when the first gas bubbles reach an elemental depth n is given by:

$$(p_{WH})_n = p_n + (D_n - D_{WH})\left[\left(\frac{dp}{dZ}\right)_{g\ mud}\right] \tag{16}$$

31

Equations (7) and (10) are used again to estimate the gas rise velocity and the real gas velocity. The simulator uses eq (10) again to calculate the time the first gas bubbles take to reach a specific elemental depth.

5.1.2. Results

The results for this case show that for a steady gas influx rate of 1 scf/sec, the first gas bubble would reach the wellhead in approximately 4.45 hours. They would expand and produce a total pit gain of 19 bbl. in those 4.45 hours. The gas volume fraction (f_g) would go up exponentially from 0.0094 at bottomhole conditions to 0.045 near the wellhead. Results also show that this gas expansion and migration would cause the wellhead pressure to go up by 72 psia, from 514 psia to 586 psia.

The pit gain, in this case, also increases exponentially, just like in the two single bubble kick cases. However, the exponential nature is less pronounced on the Pit gain vs Time plots. These plots were following the expansion of a single bubble in the first two scenarios. So, they typically showed half of the total expansion in the last quarter of the migration time. In this case, they represent the expansion of multiple bubbles along with the new gas that is coming in steadily. Hence, they show only 42% of the total increase in the last quarter. The following Figs. 5.1- 5.3 depict these results graphically.
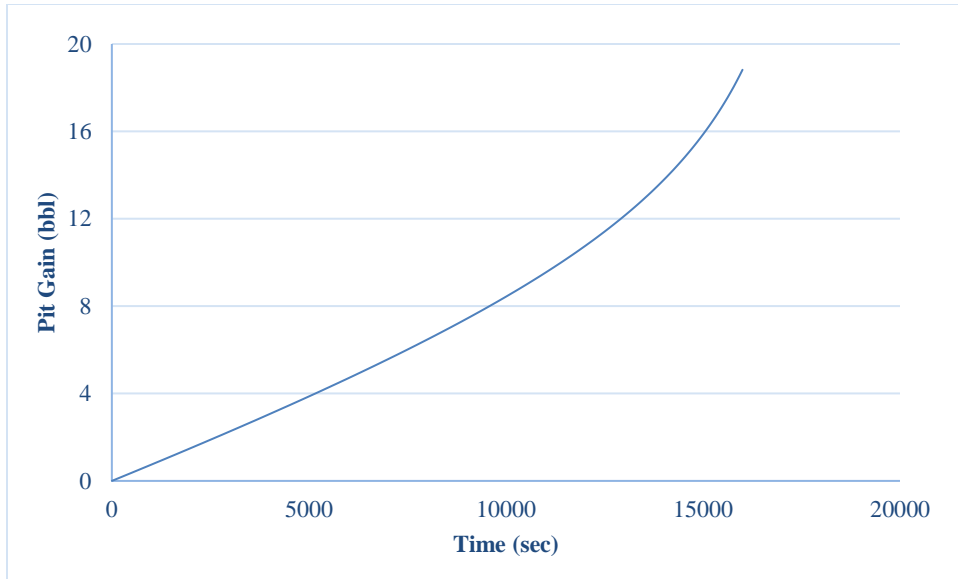
Figure 5.1 Pit gain vs Time plot for a 1 scf/sec constant gas kick influx rate.
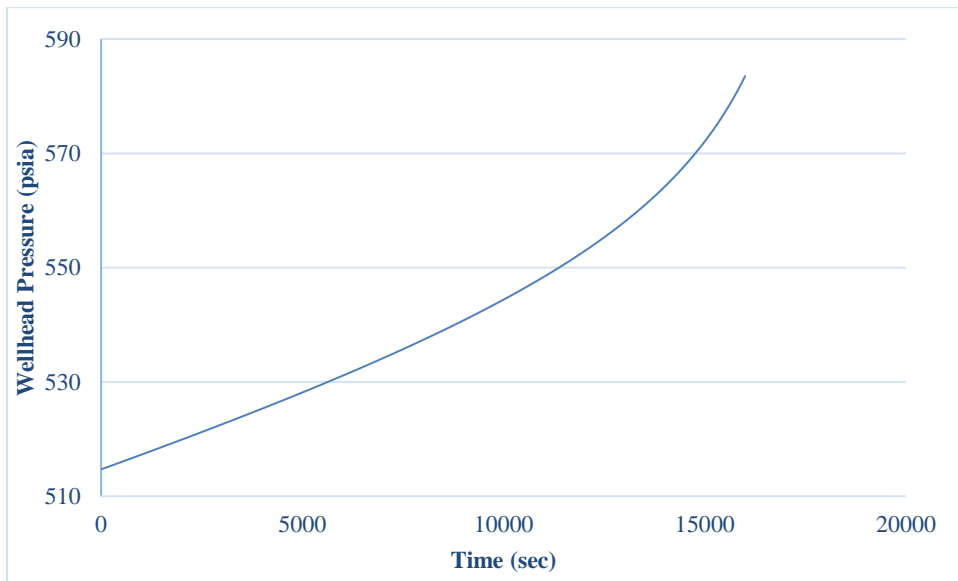
Figure 5.2 Wellhead pressure vs Time plot for a 1 scf/sec constant gas kick influx rate.
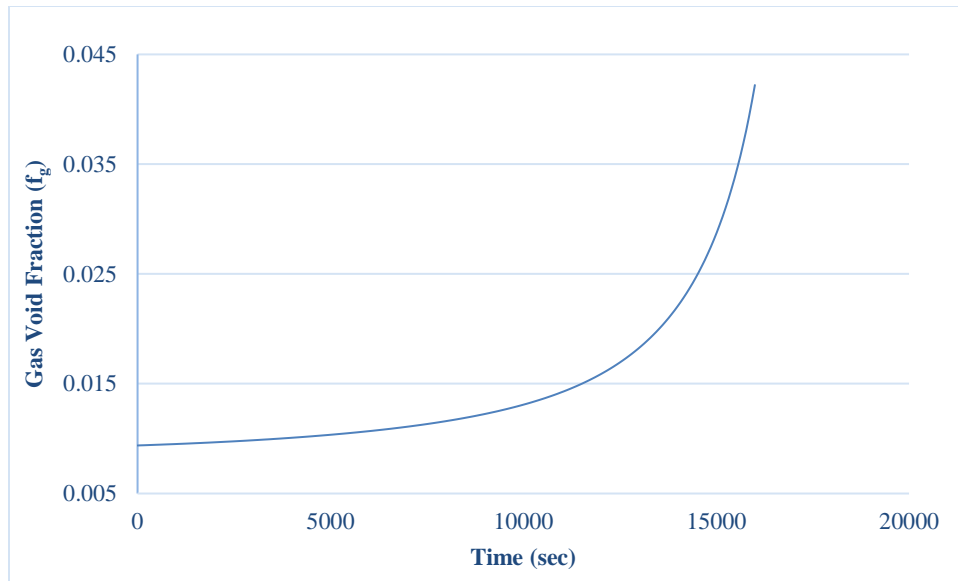
Figure 5.3 Gas void fraction (f_g) vs Time plot for a 1 scf/sec constant gas kick influx rate.

5.1.3. Sensitivity Analysis

This section compares the results for three different gas influx rates, 1-, 6-, and 12 scf/sec. All other simulator conditions, such as the well depth, mud-weight, inclination, etc. are the same as the base case. Results show that the first gas bubbles would reach the wellhead in 4.45 hours for a 1 scf/sec kick influx rate. Whereas they would only take 3.9-, and 3 hours for the flow rates of 6 scf/sec and 12 scf/sec respectively. This result is not surprising, because at higher gas influx rates, the real gas velocity, given by eq (10), would be higher. Hence the gas bubbles would reach the wellhead faster than at lower influx rates. The 1 scf/sec influx would produce a total pit gain of 19 bbl., while the other two would produce 85-, and 127 bbl.

A 1 scf/sec influx of gas would increase the wellhead pressure by approximately 72 psia in 4.45 hours. While a 6-, and 12 scf/sec influxes would increase WHP by 314-,

and 462 psia in 3.9-, and 3 hours respectively. These results are consistent with those from cases 1a, and 1b. The more gas there is in the annulus, the lighter the two-phase mixture becomes and the smaller the pressure drop between the BH and the WH. Hence, the larger increases in WH pressure at higher kick influx rates. The gas volume fraction would increase approximately fivefold for a 1 scf/sec influx between the BH and the WH. While it would increase only 2.2 times and 1.6 times for the 6-, and 12 scf/sec influxes. The Figs. 5.4- 5.6 below visualize these results:
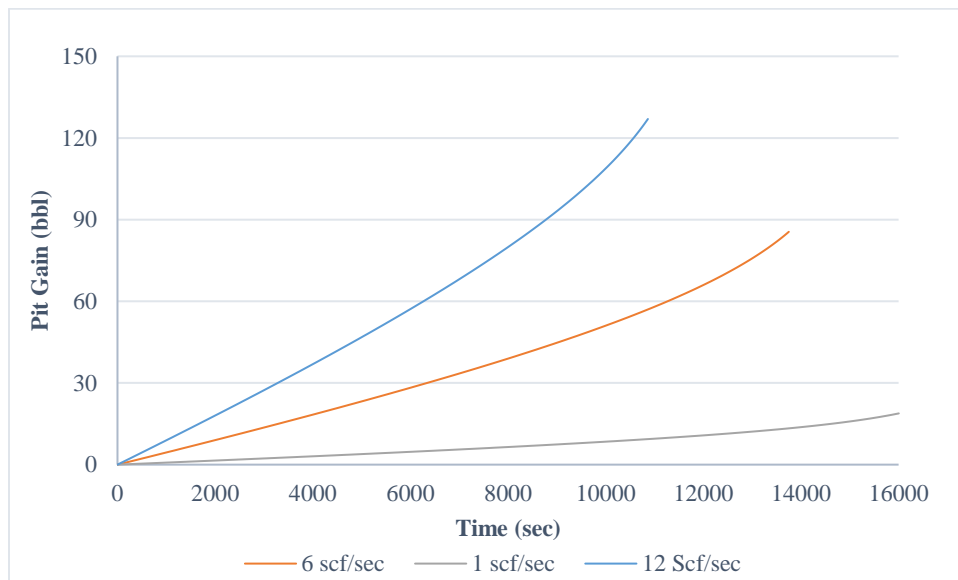
Figure 5.4 Pit gain vs Time plots comparison among different kick influx rates.
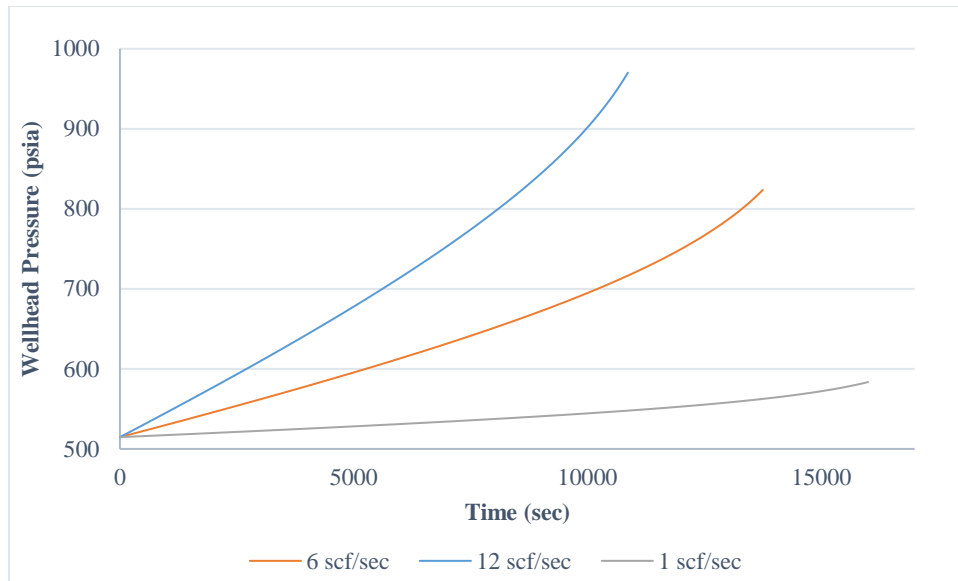
Figure 5.5 Wellhead pressure vs Time plots comparison among different kick influx rates.
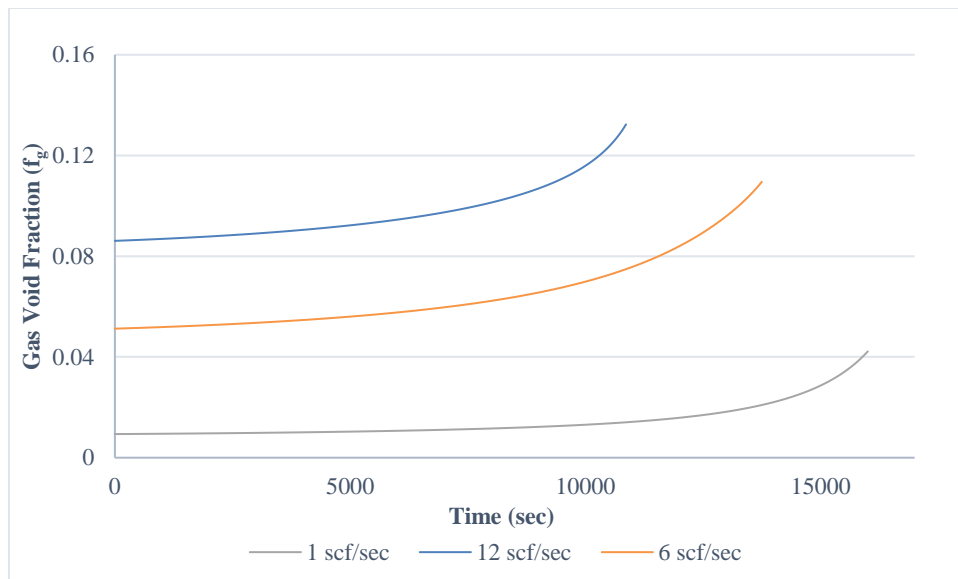
Figure 5.6 Gas void fraction (f$_g$) vs Time plots comparison among different kick influx rates.

5.2. Constant Gas Influx Kick Migration with Mud Circulation

Gas is leaking into the well at a steady rate of 1 standard cubic foot per second (scf/sec) at 10,000 ft. The drilling fluid circulation rate in the well is 702 gal/min. As the first gas molecules enter the wellbore, the initial single-phase mudflow in the annulus transitions into a two-phase flow. The flow above the first gas bubbles will still be single-phase mudflow. But the flow everywhere below the highest point reached by the gas kick, will be a two-phase flow region. This situation might arise, when a driller is trying to circulate a kick out of the well by maintaining a steady but inadequate BHP. The simulator investigates the time taken, total pit gain produced, and the change in WHP caused by the gas influx, assuming no additional mitigation attempts and a steady BHP.

5.2.1. Modeling

This case is very similar to the one discussed in the previous sub-section, except for the added drilling fluid circulation. So, the same problem in developing a pressure profile for the two-phase flow region exists. The simulator uses the step-iterative approach again to deal with this problem. All the equations used in the previous subsection except eq (16) apply for this case as well. The two-phase flow equations presented in appendix B are also applicable here without any modifications. The only difference when using these equations is in the mixture velocity. For the previous case, the mixture velocity was equal to the superficial gas velocity. But, here, the mixture velocity is the sum of the liquid phase and gas phase superficial velocities. The corrections to eq (16) to use it in this scenario are:

$$(p_{WH})_n = p_n + (D_n - D_{WH})\left[\left(\frac{dp}{dZ}\right)_{g,mud}\right] + (D_n - D_{n+1})\left\{\sum_{i=n}^{100}\left[\left(\frac{dp}{dZ}\right)_{f,mud}\right]_i\right\} \qquad (17)$$

Because there is mud circulation in the annulus, this case cannot ignore the frictional pressure drop from the drilling mud. The additional pressure gradient term in the above two equations corrects for this frictional pressure drop. Like the last situation, Equations (7) and (10) are used again to estimate the gas rise velocity and the real gas velocity. And eq (10) is used to calculate the time the first gas bubbles take to reach a specific elemental depth.

5.2.2. Results

The results for this case show that for a steady gas influx rate of 1 scf/sec, in a circulating well, the first gas bubble would reach the wellhead in approximately 52 minutes. They would expand and produce a total pit gain of 3.8 bbl. in those 52 minutes. The gas volume fraction (f_g) would go up exponentially from 0.0018 at bottomhole conditions to 0.01 near the wellhead. Results also show that this gas expansion and migration would cause the wellhead pressure to go up by 14 psia, from 506 psia to 520 psia. The Figs. 5.7- 5.9 below depict these results graphically.
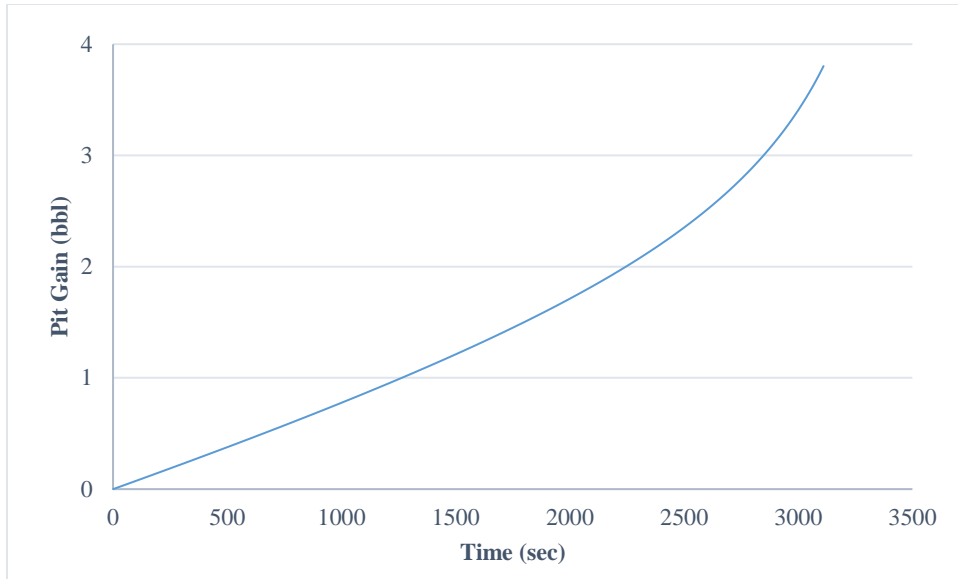
Figure 5.7 Pit gain vs Time plot for a 1 scf/sec constant gas kick influx in a circulating annulus.
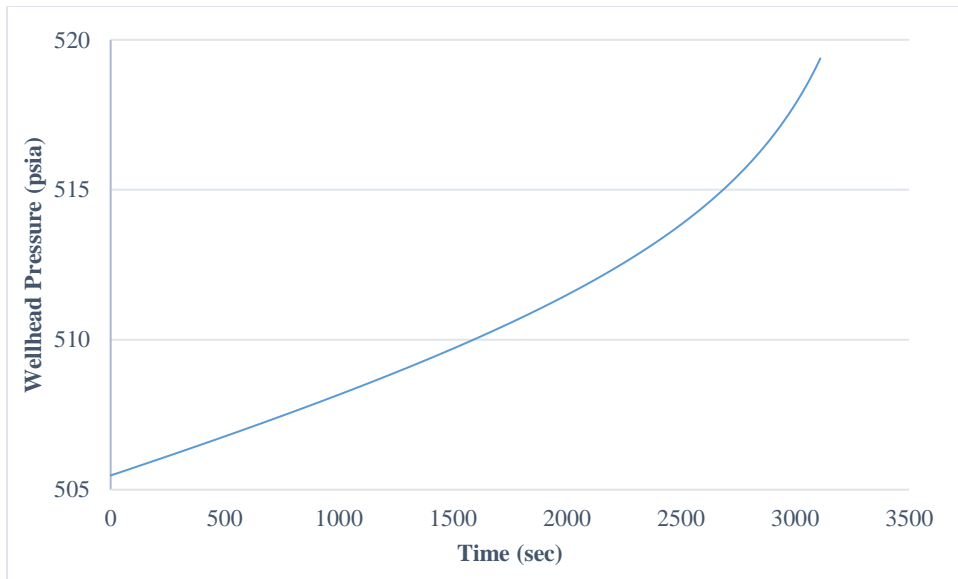
Figure 5.8 Wellhead pressure vs Time plot for a 1 scf/sec constant gas kick influx in a circulating annulus.
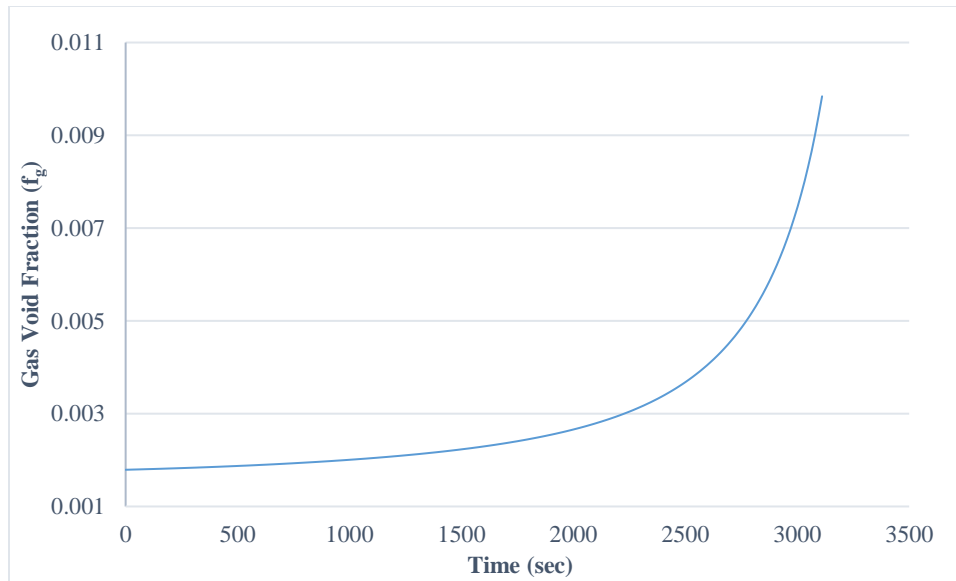
Figure 5.9 Gas void fraction (f_g) vs Time plot for a 1 scf/sec constant gas kick influx in a circulating annulus.

5.2.3. Sensitivity Analysis

This section compares the results for three different gas influx rates, 1-, 6-, and 12 scf/sec. All other simulator conditions, such as the well depth, mud-weight, inclination, etc. are the same as the base case. Results in Figs. 5.10- 5.12 show that the first gas bubbles would reach the wellhead in 52 minutes for a 1 scf/sec kick influx rate. However, unlike in the case without any circulation, the 6-, and 12 scf/sec flow rates also take very similar 51- and 50 minutes respectively. One reason for this deviance is the domination of the two-phase regime by the drilling mudflow. Unlike in the case with no mud circulation, the mixture velocity, in this case, is dominated by the drilling mud superficial velocity. Hence, the changes in the gas influx rates, while significant when there is no circulation, are not reflected in the bubble migration times. The 1 scf/sec influx would produce a total pit gain of 3.8 bbl., while the other two would produce 22-, and 41 bbl.

40

A 1 scf/sec influx of gas would increase the wellhead pressure by approximately 14 psia in 52 minutes. While a 6-, and 12 scf/sec influxes would increase WHP by 79-, and 150 psia in 51-, and 50 minutes respectively. The gas volume fraction would increase approximately six-fold for a 1 scf/sec influx between the BH and the WH. But it would increase only five times and four times for the 6-, and 12 scf/sec influxes. The graphs below visualize these results:
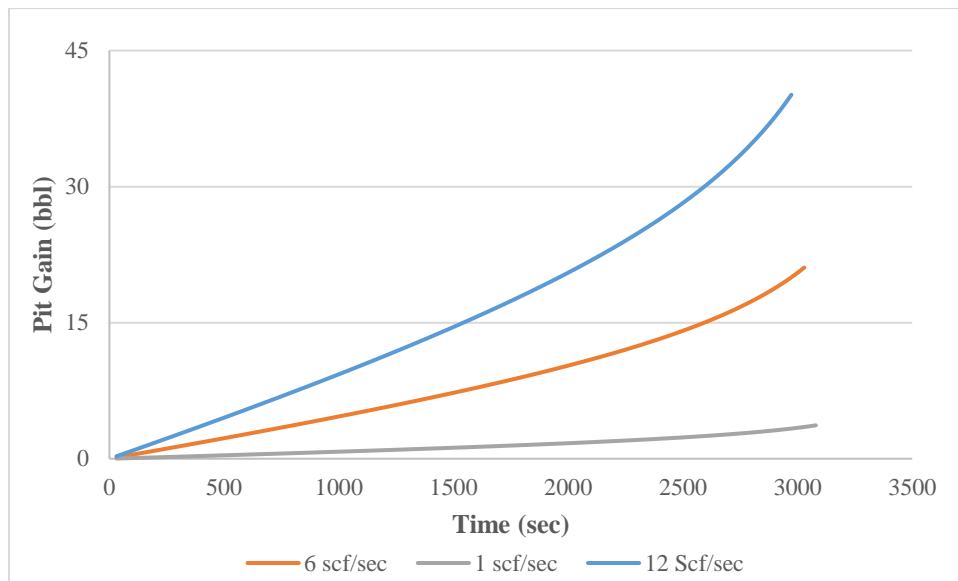
Figure 5.10 Pit gain vs Time plots comparison among different kick influx rates in a circulating annulus.
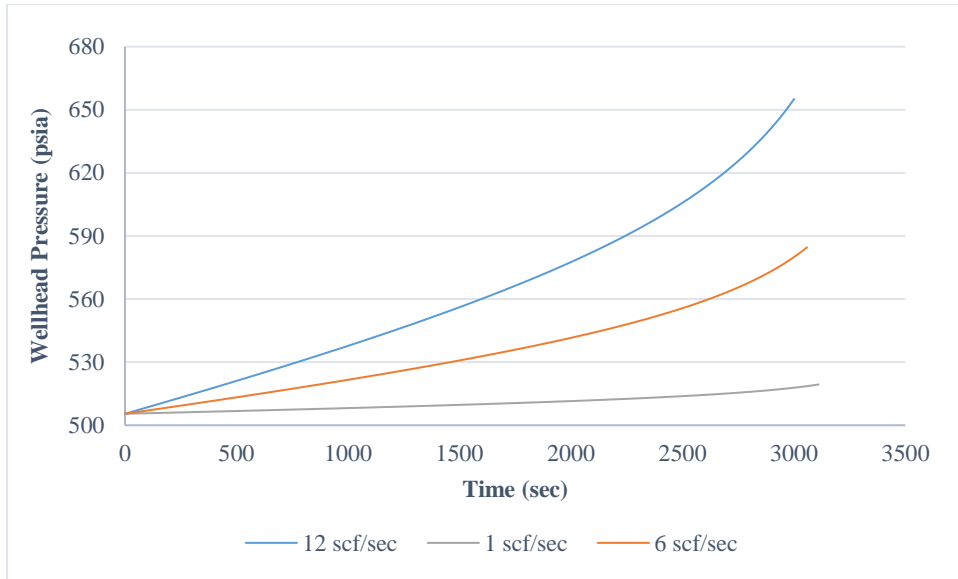
Figure 5.11 Wellhead pressure vs Time plots comparison among different kick influx rates in a circulating annulus.
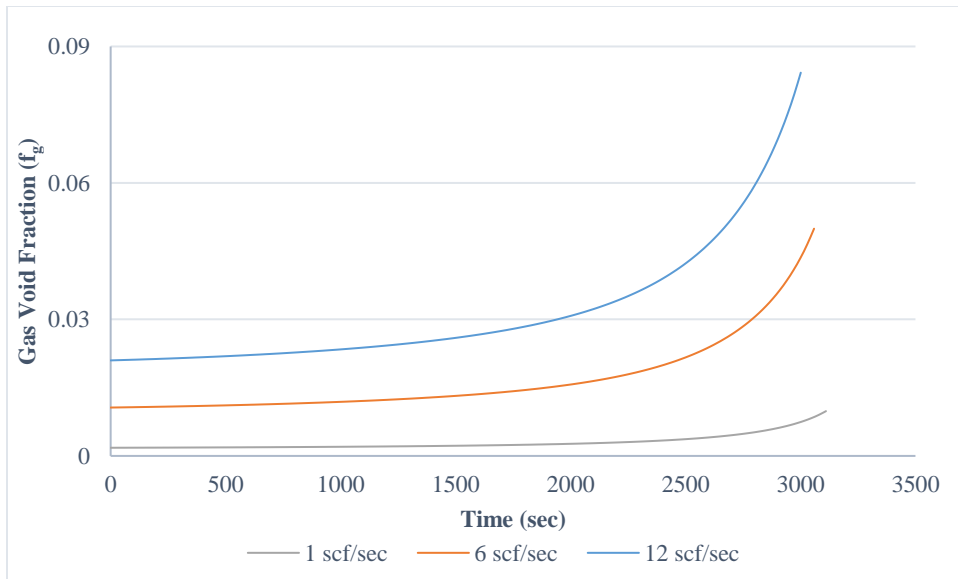
Figure 5.12 Gas void fraction (f_g) vs Time plots comparison among different kick influx rates in a circulating annulus.

5.3. Comparison between the Cases with and without Circulation

This section compares the results for the two constant gas kick influx cases, (with and without circulation in the well). The comparisons shown in Figs. 5.13- 5.18 are for two flow rates, 1-, and 12 scf/sec. The results show that when the well is circulating, the gas bubbles would reach the wellhead in less than 40% of the time it takes when it is not circulating. The two-phase mixture velocity, which is the sum of gas and liquid superficial velocities, is much higher when there is circulation. Higher mixture velocities result in lower gas void fraction (f_g) values, and consequently, lower total pit gain. Lower f_g values also mean less mud replaced by gas in the annulus, higher pressure drop, and lower wellhead pressure. The following plots show these results:
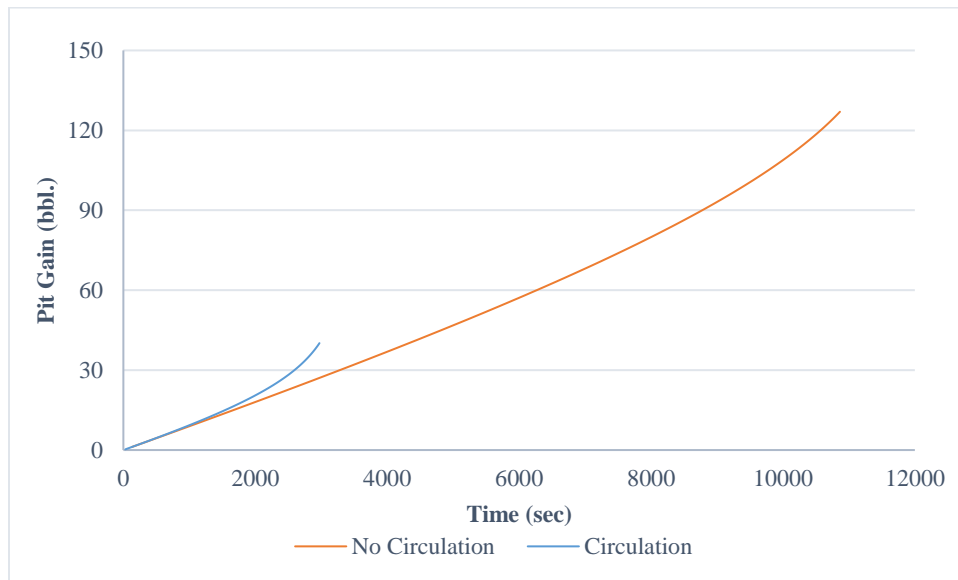
Figure 5.13 Pit gain vs Time plots comparison between the cases with and without any circulation; For a 12 scf/sec kick influx rate.
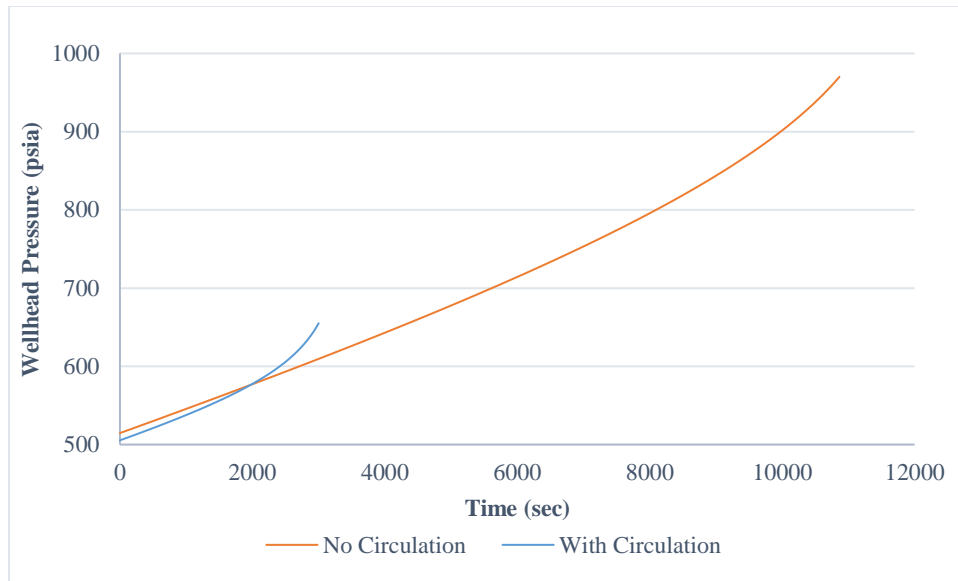
Figure 5.14 Wellhead annulus pressure vs Time plots comparison between the cases with and without any circulation; For a 12 scf/sec kick influx rate.
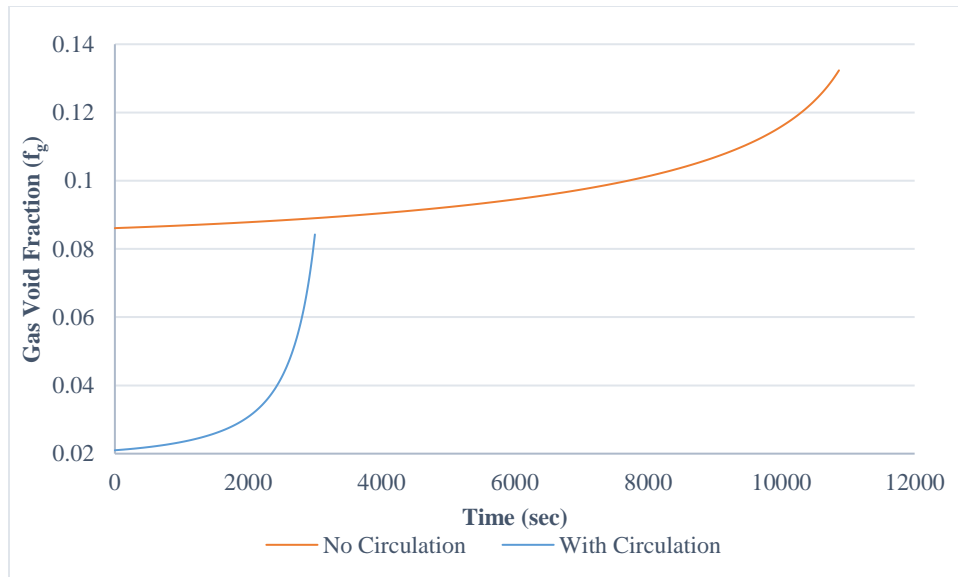
Figure 5.15 Gas void fraction (f_g) vs Time plots comparison between the cases with and without any circulation; For a 12 scf/sec kick influx rate.
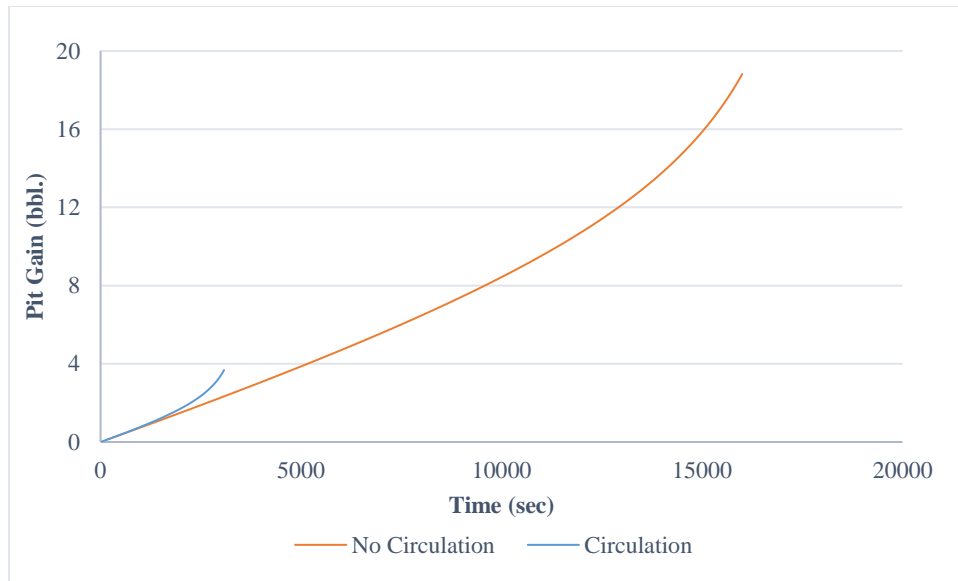
Figure 5.16 Pit gain vs Time plots comparison between the cases with and without any circulation; For a 1 scf/sec kick influx rate.
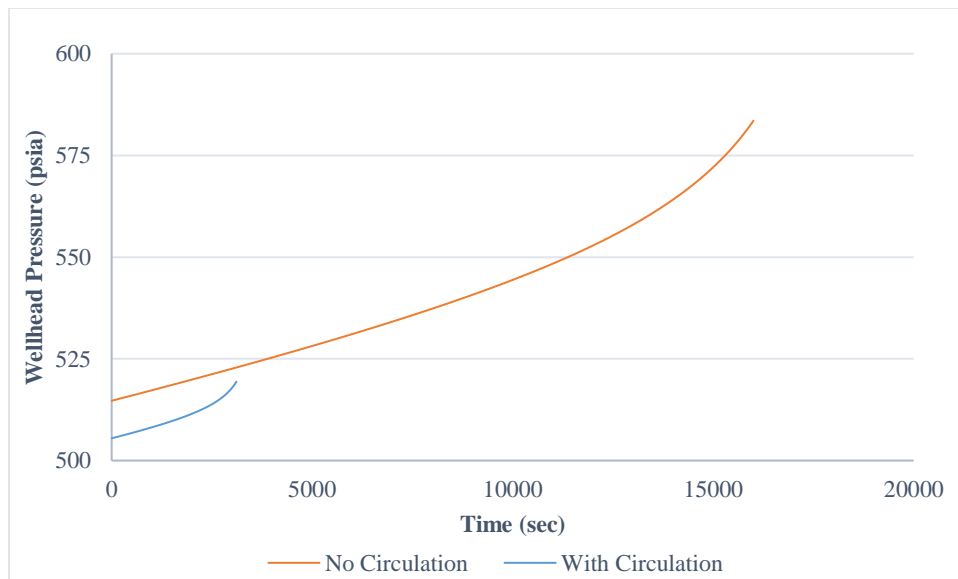
Figure 5.17 Wellhead annulus pressure vs Time plots comparison between the cases with and without any circulation; For a 1 scf/sec kick influx rate.

45
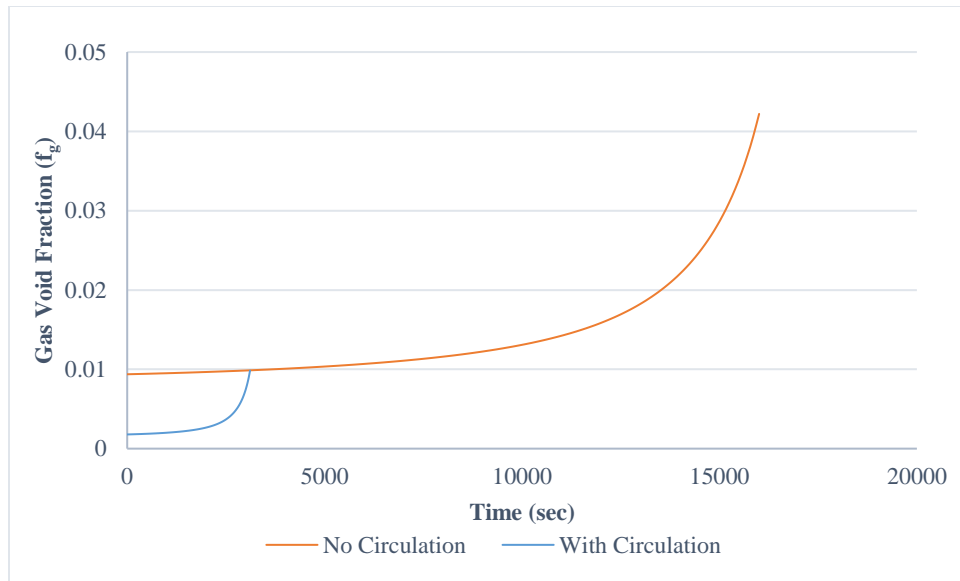
Figure 5.18 Gas void fraction (f$_g$) vs Time plots comparison between the cases with and without any circulation; For a 1 scf/sec kick influx rate.

6. METHANE SOLUBILITY IN OIL-BASED DRILLING FLUIDS[*]

The solubility of the gas kick in oil-based drilling fluids is of particular interest while modeling kick migration. The amount of free gas in the annulus determines the volume occupied by the gas kick in the annulus. It also affects the pressure at the casing shoe, and wellhead, and to some extent, the time taken by the gas bubbles to reach the wellhead. Hence, the next step in evolving the previous four models and bringing them closer to a practical scenario is to incorporate gas solubility into them. The simulator accomplishes this by using, the Peng-Robinson equation of state in conjunction with the concepts of fugacity and Van der Waal's mixing rules. It determines the mole fraction of the gas kick (methane) in the liquid mixture and calculates the solution gas-oil ratio (GOR) from this data.

6.1. Solubility Modeling

The following equation gives the chemical potential of a real fluid in terms of its fugacity:

$$dG = RT \, d(lnf) \tag{18}$$

$$\lim_{p \to 0} f = p \tag{19}$$

Where G is the Gibbs molar free energy of a pure fluid at a constant temperature. f is the fugacity, R is the real gas constant, p is the pressure, and T is the temperature. The chemical potential, G_j, for the jth component of a mixture at equilibrium must be the same in both the gas and the liquid phases. Thus, at equilibrium, the fugacities of the jth component must be equal in both the gas and the liquid phases. Thus, Gas-liquid equilibria can be calculated under the condition that:

$$f_{gj} = f_{Lj} \tag{20}$$

For all components j. In equation (20), f_{gj} is the fugacity of the jth component's gas phase. f_{Lj} is the fugacity of the jth component's liquid phase. Since this simulator assumes that the kick is pure methane, it only calculates the fugacity values gas and liquid phases of methane.

For pure substances, the fugacity coefficient is the ratio of fugacity to pressure (f/p). Fugacity coefficient is given by the following equation (McCain, 2017):

$$\ln\left(\frac{f}{p}\right) = z - 1 - \ln(z) + \int_{\infty}^{V_M} \frac{1}{RT}\left[\left(\frac{RT}{V_M}\right) - p\right] dV_M \tag{21}$$

Peng-Robinson equation of state is given by (Peng et al., 1976),

$$P = \left(\frac{RT}{V_M - b}\right) - \left(\frac{a(T)}{V_M(V_M + b) + b(V_M - b)}\right) \tag{22}$$

Where V_M is the molar volume; P, T are the pressure and temperature respectively, and a(T), b are given by the following equations:

$$a \ (T) \ = a_c \alpha(T) = \frac{0.45724R^2 {T_c}^2}{P_c} \alpha(T) \tag{23}$$

$$b = \frac{0.07780RT_c}{P_c} \tag{24}$$

Where, $\alpha(T)$ is given by,

$$(\alpha(T))^{\frac{1}{2}} = [1 + m(1 - T_{pr}^{\frac{1}{2}})] \tag{25}$$

Where, $\qquad m = 0.3796 + 1.54226\omega - 0.2699\omega^2 \tag{26}$

When $\omega \leq 0.49$

and $\qquad m = 0.3796 + 1.48503\omega - 0.1644\omega^2 + 0.016667\omega^3 \tag{27}$

When $\omega > 0.49$

Peng-Robinson equation is often re-written as,

$$Z^3 + (B - 1)Z^2 + (A - 3B^2 - 2B)Z - (AB - B^2 - B^3) = 0 \tag{28}$$

where $\qquad A = \frac{aP}{(RT)^2} \quad B = \frac{bP}{RT} \tag{29}$

McCain, 2017 presented the following integration for equation (21):

$$\ln\left(\frac{f_g}{p}\right) = z_g - 1 - \ln(z_g - B) - (\frac{A}{2^{1.5}\,B}) \ln\left(\frac{z_g + (2^{0.5} + 1)B}{z_g - (2^{0.5} - 1)B}\right)$$

and $\tag{30}$

$$\ln\left(\frac{f_L}{p}\right) = z_L - 1 - \ln(z_L - B) - (\frac{A}{2^{1.5}\,B}) \ln\left(\frac{z_L + (2^{0.5} + 1)B}{z_L - (2^{0.5} - 1)B}\right)$$

Where, z_g, z_L are gas and liquid-phase z-factors for the mixture. For the methane-drilling fluid mixture, the values of a and b in equation (29) are given by applying the Van der Waal's mixing rules. The following set of equations show these rules mathematically:

49

$$a_g = \sum_i \sum_j y_i y_j \sqrt{a_i a_j}(1 - k_{ij}) \qquad a_L = \sum_i \sum_j x_i x_j \sqrt{a_i a_j}(1 - k_{ij})$$

$$b_g = \sum_i \sum_j y_i y_j \frac{(b_i + b_j)}{2}(1 - l_{ij}) \qquad b_L = \sum_i \sum_j x_i x_j \frac{(b_i + b_j)}{2}(1 - l_{ij}) \tag{31}$$

Where x_i, x_j are the liquid phase mole fractions of the ith and j^{th} components of the mixture.

And y_i, y_j are the gas-phase mole fractions of the ith and jth components of the mixture.

a_g, b_g are the a, b values for the gas phase and a_L, b_L are the same for the liquid phase. K_{ij}

is the Binary interaction coefficient to correct for interaction between molecules and l_{ij} is

the Binary interaction coefficient to correct for volume between molecules. Feng et al.

(2019) developed two polynomial correlations for these binary interaction coefficients

from experimental data:

$$k_{ij} = a_0 + a_1 r + a_2 T + a_3 rT + a_4 r^2 + a_5 T^2$$

$$l_{ij} = b_0 + b_1 r + b_2 T + b_3 rT + b_4 r^2 + b_5 T^2 \tag{32}$$

Where r is the water-Oil ratio, and T is the temperature. The values of the constants a_0-a_5,

and b_0-b_5, as proposed by Feng et al. (2019), are shown in Table 6.1 below,

Table 6.1 Coefficients of BIC equations for a methane and oil-based mud mixture

Coefficients	a_0 (b_0)	a_1 (b_1)	a_2 (b_2)/ K^{-1}	a_3 (b_3)/ K^{-1}	a_4 (b_4)	a_5 (b_5)/ K^{-2}
k_{ij}	2.2088	0.6552	-0.0193	-6.1250E-04	-0.0358	3.0843E-05
l_{ij}	2.8371	0.0813	-0.0099	-7.2500E-04	0.0010	2.0222E-05

The simulator takes advantage of the pressure and temperature profiles developed

in the previous cases to execute solubility calculations. This thesis only presents the

solubility results for case-2b (A constant gas kick influx in a circulation annulus). So, all

the modeling discussions from this point on are referring to case-2b. The calculations start

at the assumption that 30% of all the liquid phase moles is methane. Subsequent iterations

50

with different liquid phase mole fraction values give the actual number of moles that are in solution.

The simulator uses the pressure and temperature at every elemental depth to first calculate the a(T), b, and α(T) values for all the components of the methane-mud mixture. A table showing the composition of the oil-based mud is presented in (appendix A). It then uses these values for individual components along with the mixing rules, equation (31) and (32) to calculate a, b for both the gas and liquid phases. The next step uses the a_g, and b_g values to get A, and B values for the gas phase, equation (29). The same process is repeated for the liquid phase using a_L and b_L. After obtaining the A and B values for both phases, the simulator solves the cubic equation in variable z, equation (28). The z value derived from using A and B of the gas phase is the gas phase z-factor and vice versa. The gas-phase z-factor z_g, and the liquid phase z-factor z_L are utilized in the equation set (30) to estimate the fugacity for both phases. If the fugacity values for both phases match, the initial assumption of 0.3 for methane mole fraction is correct. If they do not match, the simulator repeats the whole process with different mole fractions until the fugacity values converge. The mole fraction at which the values converge is the mole fraction of methane in the liquid phase of the mixture. The mole fraction thus calculated gives the maximum possible Gas-Oil ratio (R_s) at each elemental depth. If the incoming Gas-liquid ration (GLR) is less than or equal to the maximum R_s, then there will be no free gas. If the kick's GLR is more than the calculated R_s, then the flow rate will be proportional to the difference between GLR and R_s.

6.1.1. Results

The mole fraction calculated from the previous method is the maximum possible mole fraction (or saturation mole fraction) for methane in the liquid phase at different elemental depths. The real liquid phase mole fraction of methane depends on the kick influx rate and is not always equal to the maximum possible (saturation) value. If the calculated value is 0.5, but only 20 moles of methane is coming in for every 80 moles of drilling fluid, the real liquid phase mole fraction will be 0.2 and not 0.5. All of the incoming gas will be in solution with the mud in this example. Free gas starts to come out of the solution only when the available gas moles per cubic foot exceed the maximum possible liquid phase moles per cubic foot. This section shows the results of the phase equilibrium calculations discussed in the previous one. Figs. 6.1 and 6.2 below depict the maximum possible mole fraction of methane in the liquid phase at different positions in the well:
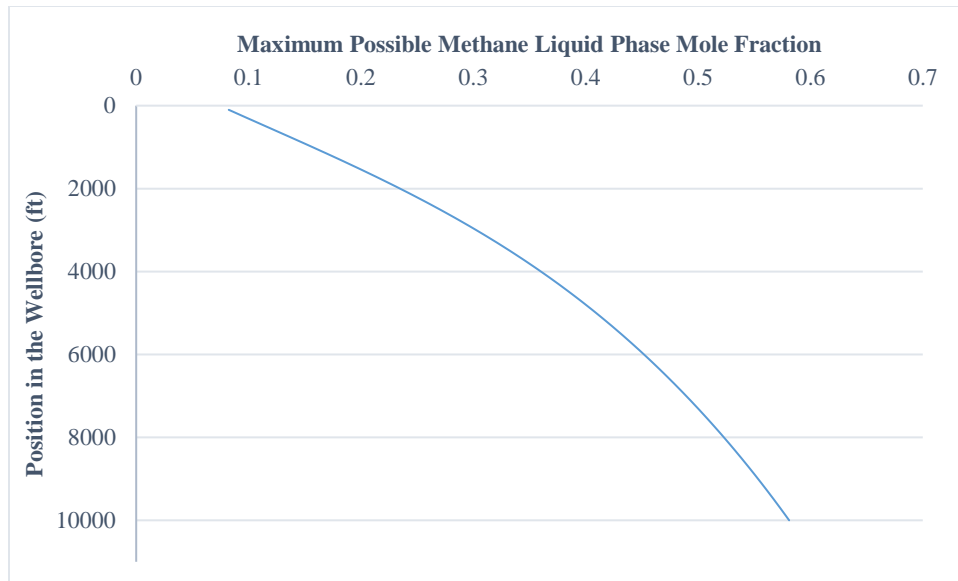
Figure 6.1 Variation in methane liquid phase mole fraction with well depth at a kick influx rate of 1 scf/sec.
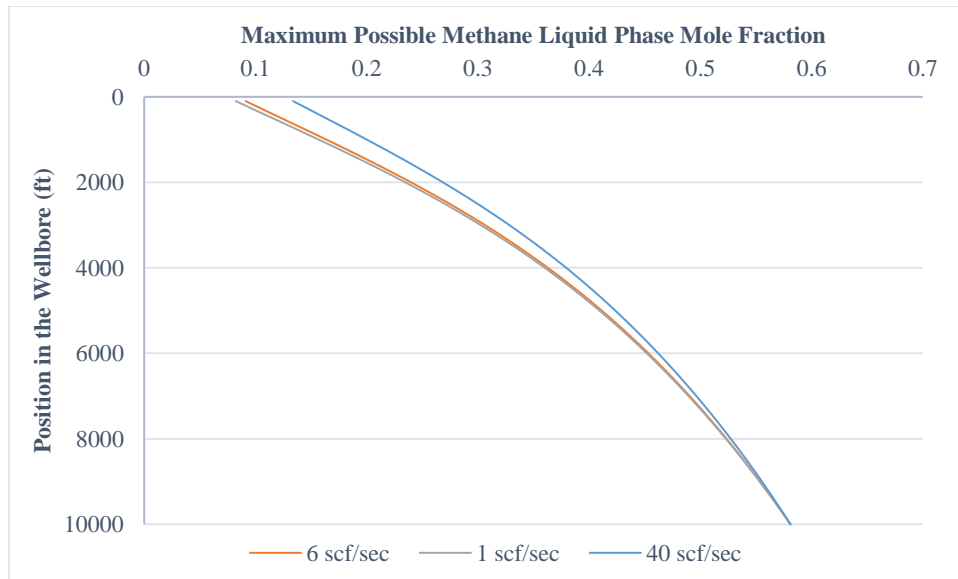
Figure 6.2 Variation in methane mole fraction with depth plots, comparison among different kick influx rates.

Results above show that the mole fraction decreases exponentially with the well depth. In other words, the amount of methane that can be in solution with the mud decreases exponentially as the mixture rises in the annulus. The temperature and pressure decrease, as the mixture rises in the annulus and hence the lower amounts of methane in solution. The results also show that at higher kick influx rates, the mixture would retain more methane in solution at shallower depths. This higher liquid phase mole fraction could be a result of higher pressures at shallow depths, caused by larger kick influx rates.

6.2. Drilling Fluid Swelling

When gas goes into solution with oil-based drilling fluid, the volume of the mud will change. The drilling fluid expands to make room for the new gas molecules entering the solution. In other words, the drilling mud "swells" because of the gas-kick dissolving in it. One way to measure the amount of swelling is the oil volume factor (B_o). B_o is the number of barrels of oil at a specific pressure and temperature required to produce one bbl. of oil at standard conditions. Many correlations are available to estimate B_o at a particular temperature and pressure. This model examined the following three correlations:

Standing, (1947)

$$B_o = 0.972 + 1.47E^{-04}\left[R_s\left(\frac{\gamma_g}{\gamma_o}\right)^{0.5} + 1.25T\right]^{1.175} \qquad (33)$$

Vasquez & Beggs, (1977)

$$B_o = 1 + 4.677E^{-4}R_s + 1.751E^{-05}(T-60)\left(\frac{\gamma_{API}}{\gamma_g}\right) - 1.811E^{-08}R_s(T-60)\left(\frac{\gamma_{API}}{\gamma_g}\right) \quad (34)$$

Petrosky & Farshad, (1993)

$$B_o = 1.0113 + 7.2046E^{-05}\left(R_s^{0.3738}\left(\frac{\gamma_g^{0.2914}}{\gamma_o^{0.6265}}\right) + 0.24626T^{0.5371}\right)^{3.0936} \quad (35)$$

The above three equations are applicable when the solution is saturated. However, when the drilling fluid is undersaturated, the following equation is used:

$$B_o = B_{ob}e^{[C_o(p_b - p)]} \quad (36)$$

where C_o is

$$c_o = \frac{-1433 + 5\,R_{sb} + 17.2\,T - 1180\,\gamma_g + 12.61\,\gamma_{API}}{10^5 p} \quad (37)$$

The drilling fluid swelling contributes to the pit gain observed at the wellhead. Because the simulator considers the pure drilling fluid compressibility to be negligible, the initial B_o is one. However, after the gas kick dissolves in the mud, B_o increases to a value more than one. In other words, one barrel of pure drilling fluid expanded to B_o barrels after forming a solution with the gas kick. Hence, the additional pit gain from drilling fluid swelling is calculated using equation (38) below.

$$(P_G)_{n+1} = (P_G)_n + \left[\left(\left\{\left(\frac{[(B_o)_{n+1} + (B_o)_n]}{2}\right) - 1\right\} + \left\{\frac{[(f_g)_{n+1} + (f_g)_n]}{2}\right\}\right)(D_{n+1} - D_n)(annular\ capacity)\right] \quad (38)$$

6.3. Results

This section discusses how the addition of gas kick solubility in drilling mud affects the results of the simulation for case-2b. The first set of results show the variation in pit gain and wellhead pressure with time for a 90 scf/sec kick influx rate. The second set shows the depth at which free gas comes out of the solution for different influx rates. These two sets of results use the B_o correlation by Petrosky & Farshad (1993). The next collection of results examines the simulation results from using the three B_o correlations. And the final set compares the results for aqueous and oil-based drilling fluids at similar kick influx rates.
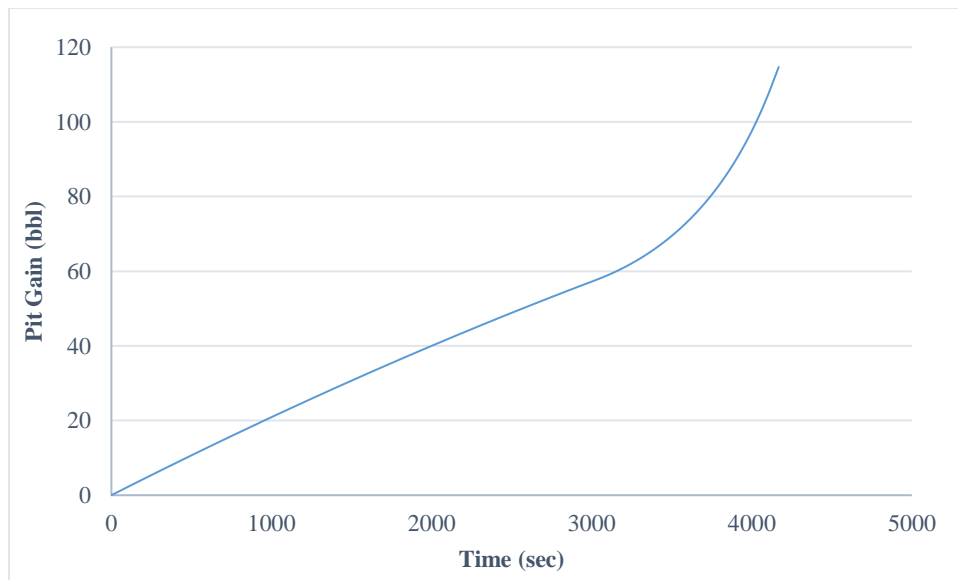
Figure 6.3 Pit gain vs Time plot for a 90 scf/sec constant gas kick influx into an oil-based mud.
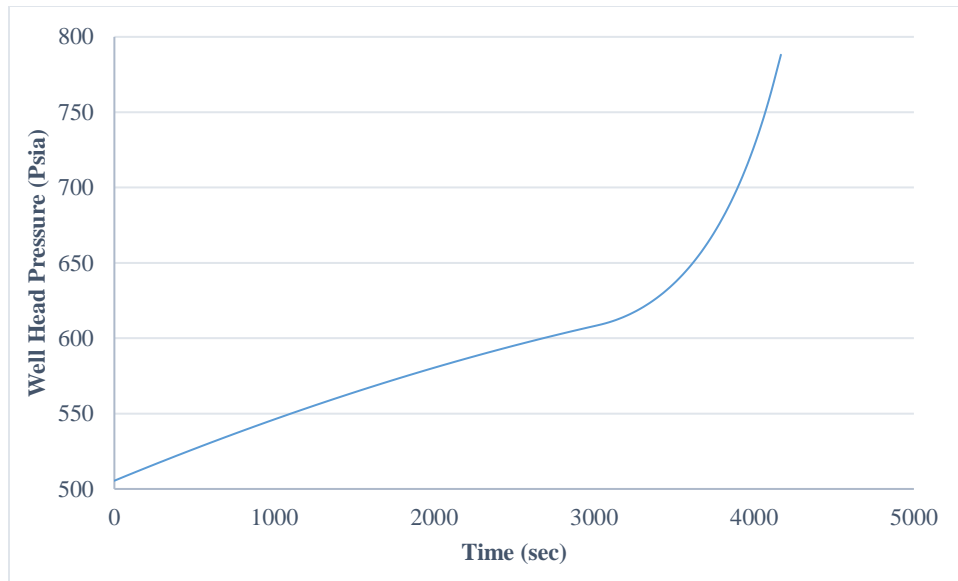
Figure 6.4 Wellhead pressure vs Time plot for a 90 scf/sec constant gas kick influx into an oil-based mud.
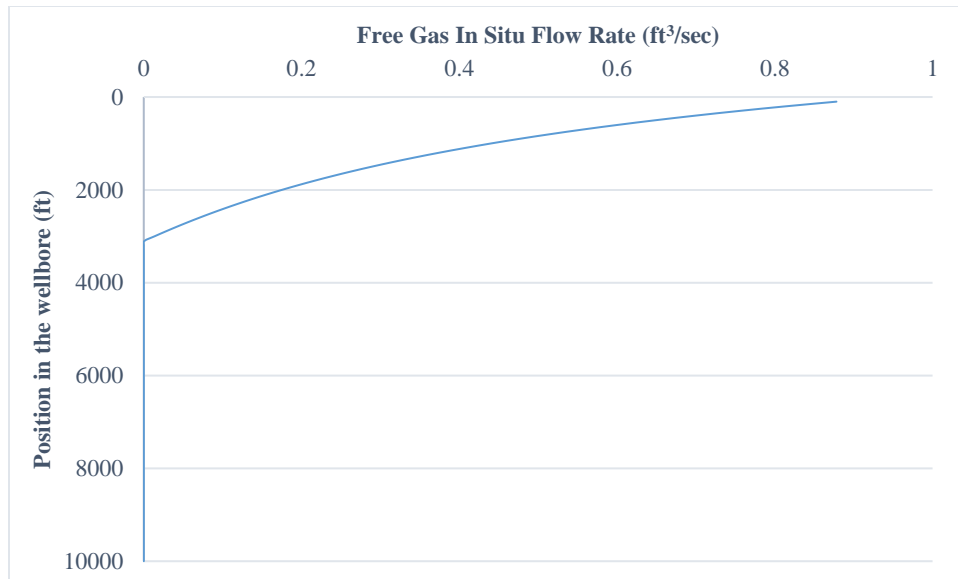
Figure 6.5 Variation in the free gas in situ flow rate with well depth for a 90 scf/sec constant gas kick influx into an oil-based mud.
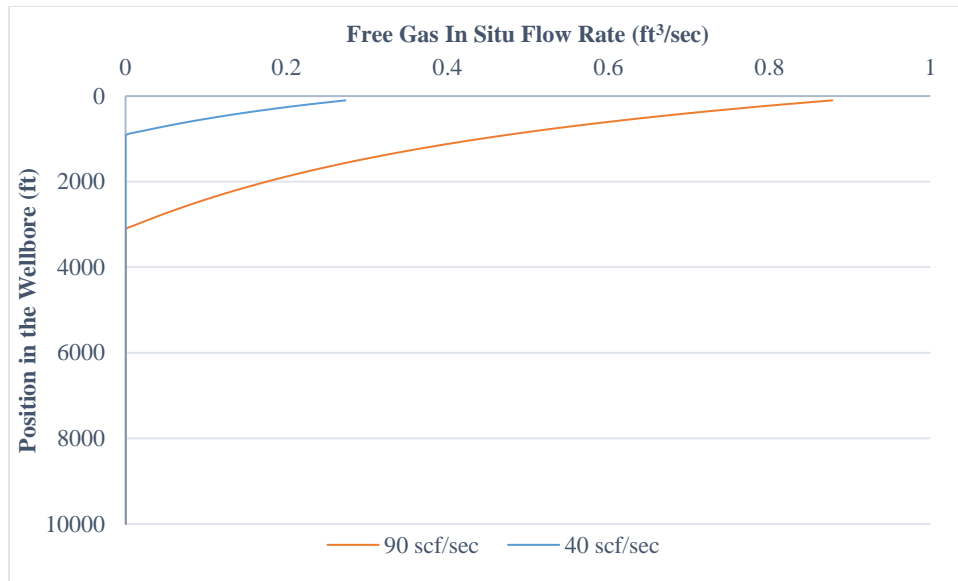
Figure 6.6 Variation in the free gas in situ flow rate with well depth plots, comparison between different flow rates.

Figures 6.3 and 6.4 show that a 90 scf/sec kick influx into a circulating oil-based mud would reach the wellhead in approximately 70 minutes. They also show that it would produce a total pit gain of 115 barrels and increase the wellhead pressure by 283 psia. Figure 6.5 shows that there will be no free gas in the annulus until the kick reaches the depth of 3200 ft. It also shows that the free gas in situ flow rate would increase exponentially with a decrease in depth after the kick reaches 3200 ft. Figure 6.6 shows that a smaller kick influx would come out of the solution at shallower depths, and the flow rate would still increase exponentially from that point on.

The appearance of free gas also accounts for the sudden increase in the slopes of the curves in figures 6.3 and 6.4. Both the pit gain and wellhead pressure plots show an abrupt increase in curve slope around the 52nd minute. This time is approximately when the first gas bubbles appear in the wellbore at 3200 ft. Free gas would replace the heavier

drilling fluid and hence increase the wellhead pressure. Free gas would also expand more than the liquid phase and thus produce more pit gain.

6.3.1. Comparison Among Different B_o Correlations

This section compares the results of the simulation from using the three B_o correlations mentioned previously. It first examines the variation in all three volume factors with the kick's position in the well, shown in Fig. 6.7. Then it compares the pit gain vs. time, and wellhead pressure vs. time plots for all three, depicted in Figs. 6.8 and 6.9. The goal of these comparisons is to find the most suitable correlation for a gas kick situation.
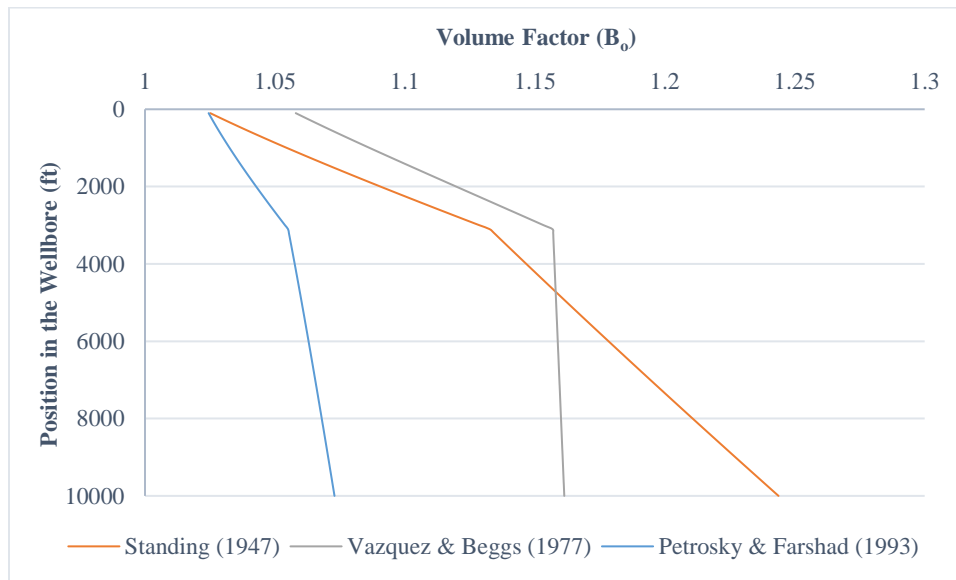
Figure 6.7 Variation in the three volume factors with the kick's position in the well for a 90 scf/sec constant gas kick influx.
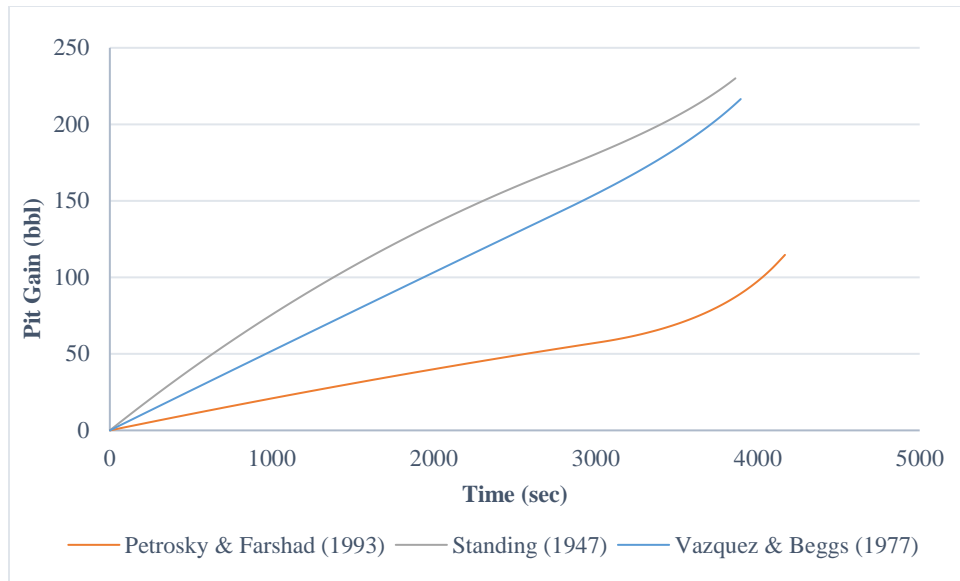
Figure 6.8 Pit gain vs Time plots comparison among different B$_o$ correlations for a 90 scf/sec constant gas kick influx.
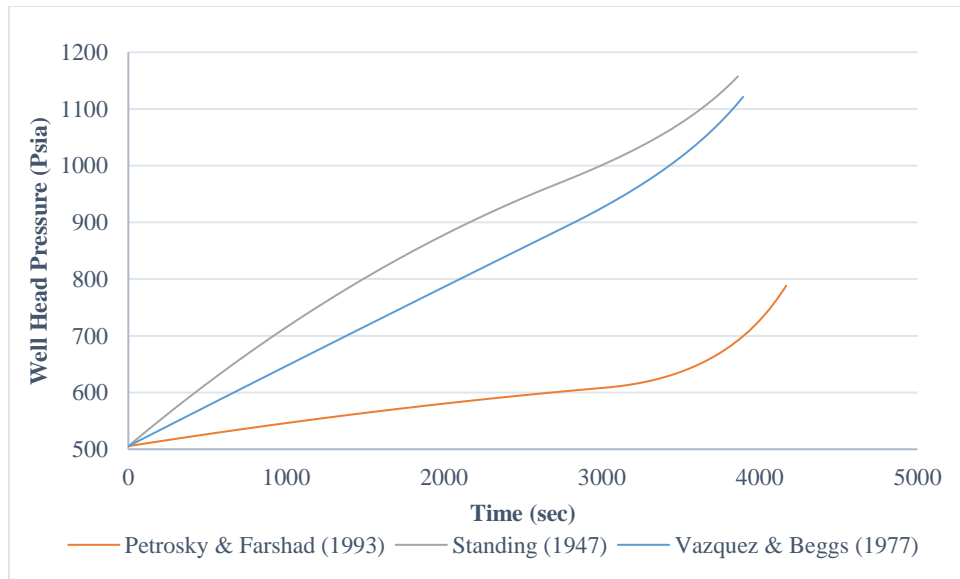
Figure 6.9 Wellhead pressure vs Time plots comparison among different B$_o$ correlations for a 90 scf/sec constant gas kick influx.

The results vary significantly with the choice of Bo correlation. Using Petrosky & Farshad (1993) correlation predicts that a 90 scf/sec kick influx would produce a total pit gain of 115 bbl. and increase the wellhead pressure by 283 psia. Whereas, using Vazquez & Beggs (1977) predicts a total pit gain of 217 bbl. and a 616 psia wellhead pressure increase. Similarly, utilizing standing (1947) correlation gives a total pit gain of 230 bbl. and a wellhead pressure increase of 652 psia. The choice of B_o affects the drilling fluid in situ flow rate, which in turn influences the time the first gas bubbles take to reach the wellhead. However, the impact of B_o on the migration time is minimal. The largest difference in the predicted time among the three correlations is less than five minutes.

6.4. Comparison between Aqueous and Oil-based Drilling Fluids

The three sub-sections below present the results of comparing the cases with water-based and oil-based muds, through Figs. 6.10- 6.15. The first sub-section presents the comparison when the Vazquez & Beggs (1977), B_o correlation is used for solubility modeling. The second and third sub-sections do the same but for Petrosky & Farshad (1993), and Standing (1947) correlations, respectively.

6.4.1. Results from Using Vazquez & Beggs (1977) Volume Factor Correlation
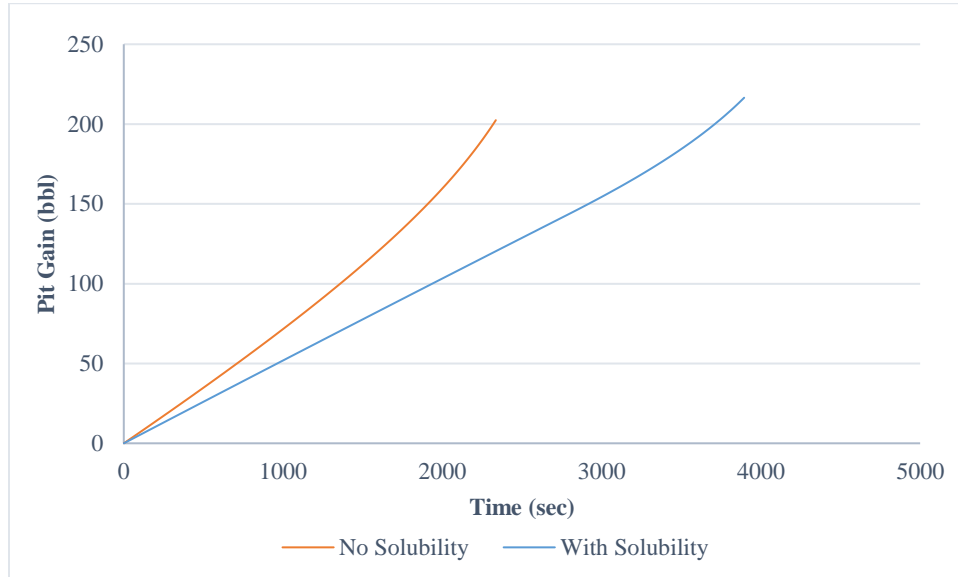
Figure 6.10 Pit gain vs Time plots comparison between the cases with OBM and WBM, for a 90 scf/sec constant gas kick influx.
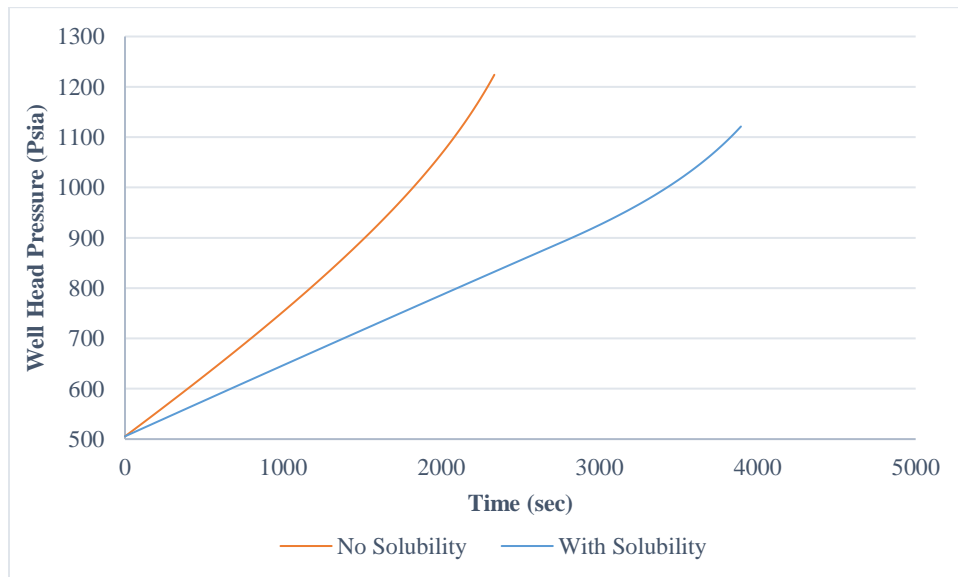
Figure 6.11 Wellhead pressure vs Time plots comparison between the cases with OBM and WBM, for a 90 scf/sec constant gas kick influx.

6.4.2. Results from Using Petrosky & Farshad (1993) Volume Factor Correlation
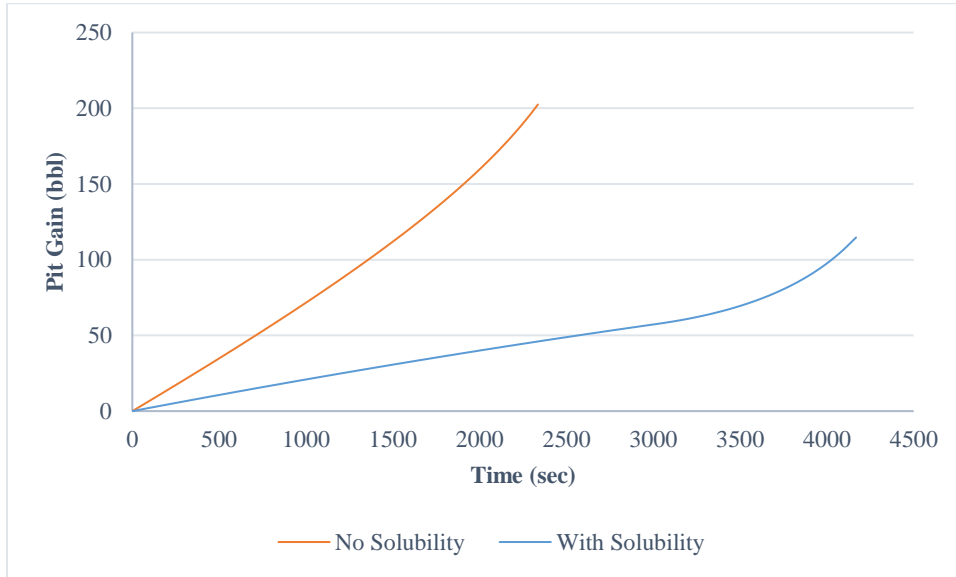
Figure 6.12 Pit gain vs Time plots comparison between the cases with OBM and WBM, for a 90 scf/sec constant gas kick influx.
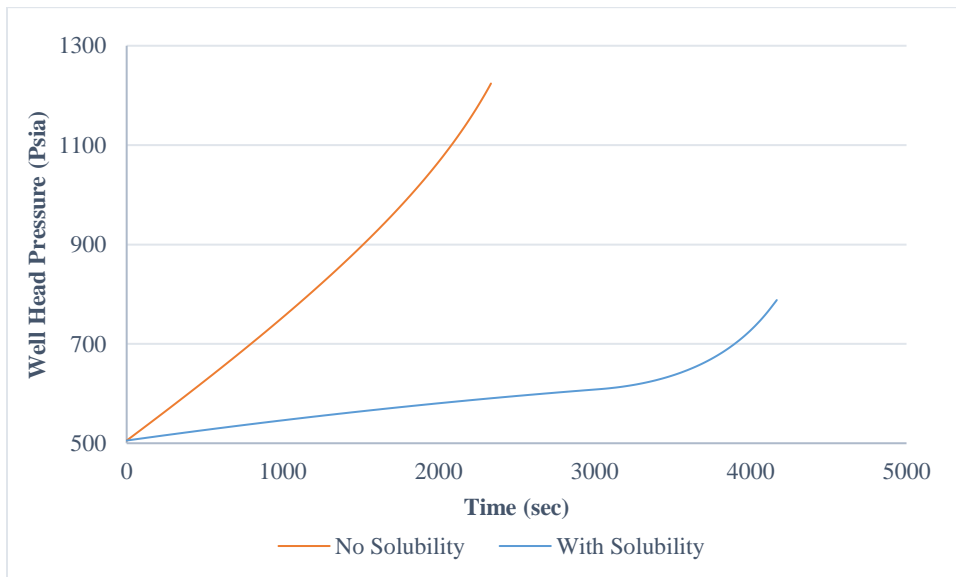
Figure 6.13 Wellhead pressure vs Time plots comparison between the cases with OBM and WBM, for a 90 scf/sec constant gas kick influx.

63

6.4.3. Results from Using Standing (1947) Volume Factor Correlation
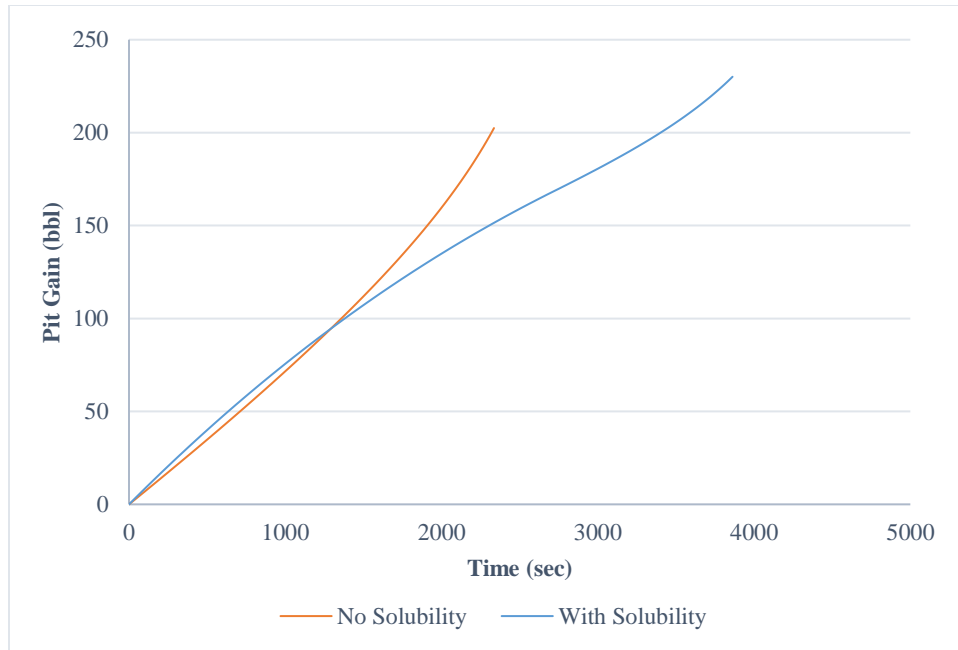
Figure 6.14 Pit gain vs Time plots comparison between the cases with OBM and WBM, for a 90 scf/sec constant gas kick influx.
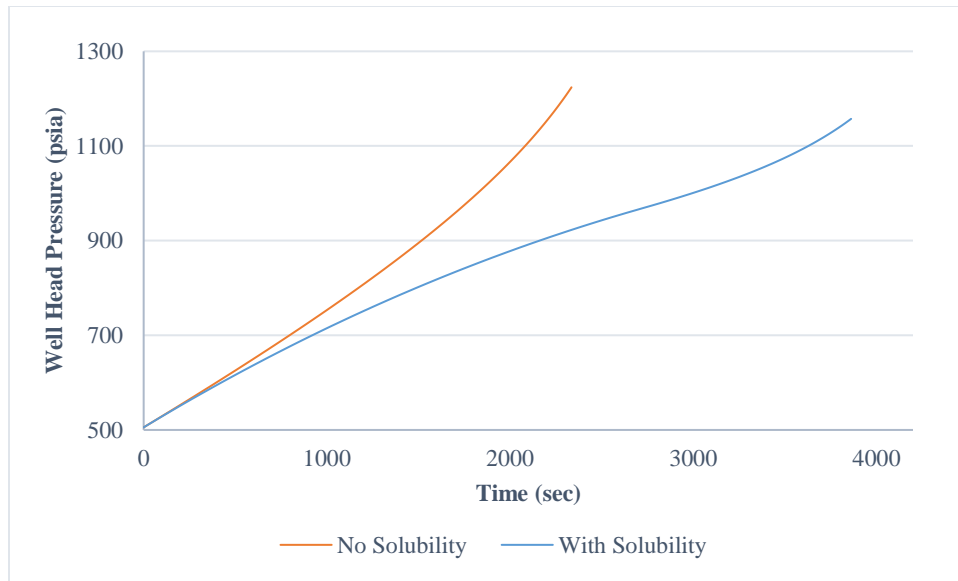
Figure 6.15 Wellhead pressure vs Time plots comparison between the cases with OBM and WBM, for a 90 scf/sec constant gas kick influx.

Figure 6.14 shows that using standing (1947) correlation gives more pit gain when the gas is soluble than when it is not, at the initial stages. In other words, using this correlation predicts that methane would occupy more volume in the liquid phase than as free gas. So, it is safe to assume that this correlation fails near this model's bottomhole conditions.

7. LIMITATIONS AND RECOMMENDATIONS FOR FUTURE WORK

All simulations in this thesis assume that the temperature at every point in the wellbore is the same as the outside temperature. They ignore the effects of heat transfer between the fluids and the surroundings. However, sudden temperature changes in offshore drilling situations make this assumption a liability to these models. Hence, future work should focus on incorporating heat transfer into these simulators.

Sections 6.3 and 6.4 show that the choice of B_o correlation has a significant impact on the final simulation results. However, most of the existing correlations are stretched beyond their limitations at the temperatures and pressures of today's offshore wells. Further research into this topic should focus on determining the best B_o correlation for gas kick-Drilling fluid mixtures. Investigations should also attempt to estimate drilling fluid swelling from EOS equations and eliminate B_o correlations completely from these models.

All the models presented here assume a constant bottomhole pressure throughout the gas migration process. However, in practice, bottomhole pressure tends to vary as a gas kick moves up in the annulus. A variable BHP would result in a fluctuating kick influx rate, which would create a transient two-phase flow system. So, future modifications to these simulators should seek to add a variable bottomhole pressure and investigate the resulting transient two-phase flow system. These models also assume the effect of drilling fluid compressibility to be negligible on the kick migration process. However, at today's deep-water well depths, it might make a tangible difference to well control operations. The kick's composition might also make a significant difference to the simulation results.

So, future research should try to account for drilling fluid compressibility along with multiple kick locations and compositions.

8. KEY OBSERVATIONS AND CONCLUSIONS

This last section briefly summarizes the observations made and conclusions drawn from investigating all the different scenarios presented in this thesis.

- Consistent with current literature and field observations, a gas kick that was migrating as a single bubble exhibited rapid expansion towards the end of its migration.

- Also consistent with previous results, this rapid expansion produced a sudden increase in wellhead pressure, which could be hazardous to the drilling equipment, and the rig.

- The kick's shape and annular geometry had a significant influence on its rise velocity and hence the migration time.

- When the kick is coming in at a constant rate, the influx rate is also critical. The influx rate dictates the two-phase flow regime in the annulus, which in turn determines the migration times and the time a driller has to take well control measures.

- The changes in pit gain and wellhead pressure are much more noticeable when there is a constant influx, making it more conspicuous than a single bubble kick.

- Gas kicks are most threatening when the driller is using an oil-based mud. A similar kick influx rate in an OBM produced less pit gain and took longer to travel the well length than in a WBM. Kick in an OBM also had a more pronounced rapid

expansion towards the end, making it insidious, and hence more dangerous than kicks in WBM.

- The choice of volume factor correlation greatly influenced the pit gain results in the OBM case. So, further investigation is needed to determine the best B_o correlation for gas kick modeling.

REFERENCES

Beggs, D. H., & Brill, J. P. (1973, May 1). A Study of Two-Phase Flow in Inclined Pipes. Society of Petroleum Engineers. doi:10.2118/4007-PA

Chandrasekaran, Sridharan, and Govindarajan Suresh Kumar. "Numerical Modeling of Real-Time Gas Influx Migration in Vertical Wellbores During Drilling Operation." International Journal of Energy for a Clean Environment, vol. 20, no. 2, 2019, pp. 95–111., doi:10.1615/interjenercleanenv.2019029547.

Chukwudi, O., Stanley, I., Boniface, O., & Stanley, O. (2018, August 6). A Realistic Kick Simulator for Casing Design - Part 2: Well Design and Execution. Society of Petroleum Engineers. doi:10.2118/193390-MS

Deepwater Horizon – BP Gulf of Mexico Oil Spill. (2017, April 19). Retrieved from https://www.epa.gov/enforcement/deepwater-horizon-bp-gulf-mexico-oil-spill

Feng, Jian & Fu, Jianhong & Chen, Ping & Xu, Liqun. (2019). Investigation of Methane/Drilling Mud Phase Behavior and its Influence to Hydrocarbon Drilling Activity. Energy Science & Engineering. 7. 10.1002/ese3.345.

Harmathy, T. Z. (1960). Velocity of Large Drops and Bubbles in Media of Infinite or Restricted Extent. AIChE Journal, 6(2), 281-288. doi:10.1002/aic.690060222

Hasan, A. R., and C. S. Kabir. Fluid Flow and Heat Transfer in Wellbores. Society of Petroleum Engineers, 2018.

Hasan, A., & Kabir, C. (1992). Two-Phase Flow in Vertical and Inclined Annuli. International Journal of Multiphase Flow, 18(2), 279-293. doi:10.1016/0301-9322(92)90089-y

Johnson, A. B., & White, D. B. (1991, December 1). Gas-Rise Velocities During Kicks. Society of Petroleum Engineers. doi:10.2118/20431-PA

Kaldirim, O., & Schubert, J. J. (2017). An Experimental Study on Riser Gas Behavior for Dual Gradient Drilling. Paper presented at the IADC/SPE Managed Pressure Drilling & Underbalanced Operations Conference & Exhibition, Rio de Janeiro, Brazil. https://doi.org/10.2118/185297-MS

Kaldirim, O., & Schubert, J. J. (2018). Experimental Study on Riser Gas Expansion and Unloading. Paper presented at the SPE/IADC Managed Pressure Drilling and Underbalanced Operations Conference and Exhibition, New Orleans, Louisiana, USA. https://doi.org/10.2118/190004-MS

Kwak, T., & Mansoori, G. (1986). Van der Waals Mixing Rules for Cubic Equations of State. Applications for Supercritical Fluid Extraction Modelling. Chemical Engineering Science, 41(5), 1303-1309. doi:10.1016/0009-2509(86)87103-2

Ma, Z., Vajargah, A. K., Chen, D., van Oort, E., May, R., MacPherson, J. D., … Curry, D. (2018, March 6). Gas Kicks in Non-Aqueous Drilling Fluids: A Well Control Challenge. Society of Petroleum Engineers. doi:10.2118/189606-MS

Manikonda, K., Hasan, A. R., Kaldirim, O., Rahmani, N., & Rahman, M. A. (2020). Estimating Swelling in Oil-based Mud due to Gas Kick Dissolution. American

Society of Mechanical Engineers-Ocean, Offshore & Arctic Engineering 2020. OMAE2020-18115

Manikonda, K., Hasan, A. R., Kaldirim, O., Schubert, J. J., & Rahman, M. A. (2019, October 13). Understanding Gas Kick Behavior in Water and Oil-Based Drilling Fluids. Society of Petroleum Engineers. doi:10.2118/198069-MS

McCain, William D. The Properties of Petroleum Fluids. PennWell, 2017.

Michael, O. C., Ugochukwu, I. S., Boniface, O., Chibunma, A., & Stephen, N. (2017, July 31). A Realistic Kick Simulator for Casing Design-Part 1. Society of Petroleum Engineers. doi:10.2118/189167-MS

Monteiro, E. N., Ribeiro, P. R., & Lomba, R. F. T. (2010, March 1). Study of the PVT Properties of Gas--Synthetic-Drilling-Fluid Mixtures Applied to Well Control. Society of Petroleum Engineers. doi:10.2118/116013-PA

O'Bryan, P. L., Bourgoyne, A. T., Jr., Monger, T. G., & Kopcso, D. P. (1988). An Experimental Study of Gas Solubility in Oil-Based Drilling Fluids. SPE Drilling Engineering, 3(01), 33-42. doi:10.2118/15414-PA

Peng, D., & Robinson, D. B. (1976). A New Two-Constant Equation of State. Industrial & Engineering Chemistry Fundamentals, 15(1), 59-64. doi:10.1021/i160057a011

Petrosky, G., & Farshad, F. (1993). Pressure-Volume-Temperature Correlations for Gulf of Mexico Crude Oils. Proceedings of SPE Annual Technical Conference and Exhibition. doi:10.2523/26644-ms

Rader, D. W., Bourgoyne, A. T., & Ward, R. H. (1975, May 1). Factors Affecting Bubble-Rise Velocity of Gas Kicks. Society of Petroleum Engineers. doi:10.2118/4647-PA

Redlich, O., and Kwong, J.N.S., 1949. On the Thermodynamics of Solutions. V. An Equation of State. Fugacities of Gaseous Solutions. Chemical Reviews 44 (1). American Chemical Society: 233&-44. doi:10.1021/cr60137a013.

Skalle, P., Podio, A. L., & Tronvoll, J. (1991, January 1). Experimental Study of Gas Rise Velocity and Its Effect on Bottomhole Pressure in a Vertical Well. Society of Petroleum Engineers. doi:10.2118/23160-MS

Standing, M. B. (1947, January 1). A Pressure-Volume-Temperature Correlation for Mixtures of California Oils and Gases. American Petroleum Institute.

Thomas, D. C., Lea, J. F., & Turek, E. A. (1984, June 1). Gas Solubility in Oil-Based Drilling Fluids: Effects on Kick Detection. Society of Petroleum Engineers. doi:10.2118/11115-PA

Vazquez, M., & Beggs, H. D. (1977). Correlations for Fluid Physical Property Prediction. SPE Annual Fall Technical Conference and Exhibition. doi:10.2118/6719-ms

Yarborough, L. 1978. Application of a Generalized Equation of State to Petroleum Reservoir Fluids, Amer. Chem. Soc. 182: 386–439.

Zuber NN, Findlay JA. Average Volumetric Concentration in Two-Phase Flow Systems. ASME. J. Heat Transfer. 1965;87(4):453-468. doi:10.1115/1.3689137.

APPENDIX A

WELL DATA

Measured Depth	10,000 ft
TVD	10,000 ft
Deviation from vertical	0°
Inclination	90°
Drill Pipe Weight	16.6 lbm/ft
Casing weight	68 lbm/ft
Casing Length	4000 ft
Hole Size	12.415 in.
Drill Pipe outside diameter	4.5 in.
Drill Pipe inside diameter	3.826 in.
Casing Outside diameter	13.375 in.
Casing Inside diameter	12.415 in.
Circulation Rate	702 gal/min
Original Mud Weight	10 lbm/gal
Surface Temperature	50 °F
Geothermal temperature Gradient	0.025 °F
Bottomhole Temperature	302 °F
Mud viscosity at BH conditions	0.39 cp
Mud viscosity at WH conditions	0.64 cp
Gas viscosity at BH conditions	0.022 cp
Gas viscosity at WH conditions	0.017 cp

APPENDIX B

DRILLIING FLUID COMPOSITION DATA

Oil-based Mud Composition Data

Component	Mole fraction	Molecular weight (lbm/lbmol)
$C_{11}H_{24}$	7.58%	156
$C_{13}H_{28}$	11.90%	184
$C_{15}H_{32}$	21.94%	212
$C_{13}H_{24}$	13.28%	180
$C_{14}H_{26}$	21.09%	194
$C_{15}H_{28}$	7.86%	208
$C_{16}H_{26}O_3$	6.34%	266
H_2O	10.00%	18